UNIVERSITY OF SOUTHAMPTON

A STUDY OF A PLATINUM ELECTROPLATING BATH

by

Adrian John Gregory BSc.

A thesis submitted for the degree of

MASTER OF PHILOSOPHY

December 1991

Department of Chemistry

UNIVERSITY OF SOUTHAMPTON

ABSTRACT

FACULTY OF SCIENCE

CHEMISTRY

Master of Philosophy

A STUDY OF A PLATINUM ELECTROPLATING BATH

by Adrian John Gregory.

Three platinum complexes, $[Pt(NH_3)_4]^{2+}$, $[Pt(H_2O)_4)]^{2+}$ and cis-$[Pt(NH_3)_2(H_2O)_2]^{2+}$ have been prepared and characterised. Voltammetry at microelectrodes has been used to investigate the reduction of the Pt(II) species and it has been shown that good quality electrodeposits can be obtained from their solutions.

The complex $[Pt(NH_3)_4]^{2+}$, in a phosphate buffer at pH 10, is marketed as an electroplating solution. Voltammetry at a platinum microdisc electrode confirmed previous work that this complex does not reduce directly in aqueous solutions. Indeed, no reduction is observed at 293 K. At temperatures above 343 K, however, a reduction peak was observed indicating the deposition of platinum. The rate of production of the electroactive species followed an Arrhenius relationship with an energy of activation of 116 kJ mol^{-1}. It is proposed that the reducible species is the product of a ligand substitution reaction at the kinetically inert d^8 metal centre; the electroactive species could be $[Pt(H_2O)_4)]^{2+}$. Electrodeposition of platinum onto a 12.5 cm^2 copper panel was investigated. Above 363 K, bright deposits at 100% current efficiency were achieved for deoxygenated solutions. Below this temperature a black deposit formed on the cathode with current efficiences of below 20%.

The chemistry and electrochemistry of $[Pt(H_2O)_4)]^{2+}$ was also studied. This complex was not stable at or above pH 1 when a precipitate of a black solid containing platinum was formed. Voltammetry using microelectrodes showed that $[Pt(H_2O)_4)]^{2+}$ at pH 0 reduced directly with a simple, diffusion limited wave. The diffusion coefficient at 294 K was found to be 8.6×10^{-6} cm^2 s^{-1} and the energy of activation for diffusion 20 kJ mol^{-1}. These results indicate that $[Pt(H_2O)_4)]^{2+}$ could indeed be the electroactive intermediate in the commercial plating bath containing $[Pt(NH_3)_4]^{2+}$. Electrodeposition from solutions of $[Pt(H_2O)_4)]^{2+}$ in perchloric acid gave bright platinum deposits at high current efficiencies even at 293 K, indicating the potential use of this solution, as an electroplating bath, in its own right.

Acknowledgements

I would like to thank my supervisor, Dr. Derek Pletcher, for his continual help and encouragement throughout this long year. If I ever tried his patience (and I must have) he never let me know of it. Similarly, I am indebted to Dr. William Levason for the considerable time he spent recording the NMR spectra and his helpful comments on the preparation of the various complexes.

The Pletcher research group, with whom I have worked at Southampton, have also been a great help both on the practical and the lighter side of things. Special thanks go to Mrs Carole Chatley, who helped and advised with the word-processing of this thesis.

I would also like to acknowledge the gift of chemicals from Johnson Matthey, without whom this expensive chemistry would not have been possible.

Finally

I dedicate this thesis to my parents
who have always been there.

CHAPTER 1

CHAPTER 2

CHAPTER 3

1. INTRODUCTION

1.1. Electroplating

1.1.1. Electroplating as a metal coating technique

Electroplating is the process of depositing a metallic coating onto a conducting substrate by electrolysing a molten salt or a solution of a metal complex [1]. If the complexes of more than one metal are reduced simultaneously a metal alloy is formed. In addition, metal coatings containing finely dispersed solid compounds, composites, can be formed by using a bath containing suspensions of the particles.

The purpose of the coating is to change the properties of the surface chemically and/or physically;

Chemically - The surfaces resistance to chemical corrosion (e.g. oxidation) may be increased or the deposited metal may make the surface catalytically active.

Physically - The surfaces resistance to physical corrosion (e.g. continuous wear) may be increased as may
surface reflectivity (e.g. for decorative purposes),
electrical conductivity (e.g. on printed circuit boards),
magnetic susceptibility (e.g. for digital data storage).

Alternatively other finishing techniques can be used to give objects metal coatings;

Electroless deposition
Chemical vapour deposition (CVD)
Physical vapour deposition (PVD)
Molten metal methods - hot dipping, rolling, spraying

Molten metal methods are only of use for relatively thick coatings of a low melting point metal onto a simply shaped object (usually sheet metal).

Both physical and chemical vapour deposition methods can cope with

shapes and deposit thin coatings on non-conducting substrates. The energy needed to do this is dependant on the boiling point of the metal or metal salt. Additionally, the vapour will be non-selective, depositing on any cooler surface.

Electroless deposition involves reducing the metal complex to the metal with an added reducing agent which is consumed as the metal is deposited. This technique offers a particularly even coating with a low porosity but it is more expensive than electroplating due to the need for specialist chemicals and the heating of the bath.

Electroplating has the following important advantages [2];

1) Operating temperatures generally lie in the range 293 - 343 K. Thus extreme temperatures, which may lead to distortion or adverse metallurgical changes, are avoided.
2) Under suitable conditions the coating adhesion is very strong
3) Often a relatively thin coating produces a radically improved surface with respect to its engineering performance.
4) It is often possible to automate the process.
and the following disadvantages

1) The rate of deposition is usually much lower than 75 $\mu m\ hour^{-1}$, unless forced electrolyte convection is used.
2) The substrate must be electrically conducting.
3) The physical size of the plating bath may limit the dimensions of the workpiece.
4) In some cases the pre-treatment liquors and / or plating bath may be toxic and require treatment before being discharged as effluent.

The advantages have ensured that electroplating has become a widely used coating process. The aim of electroplating, however, - to reproducibly deposit a uniform thickness of adherent metal with the desired properties - is not easy. Different sizes and geometries of the workpiece may need different parameters to obtain the same finish with the same metal bath. Thus it is necessary to qualitatively understand how each parameter in the plating process affects the deposited layer.

1.1.2. The electroplating bath

A typical electroplating bath is shown in figure 1.01 [3].

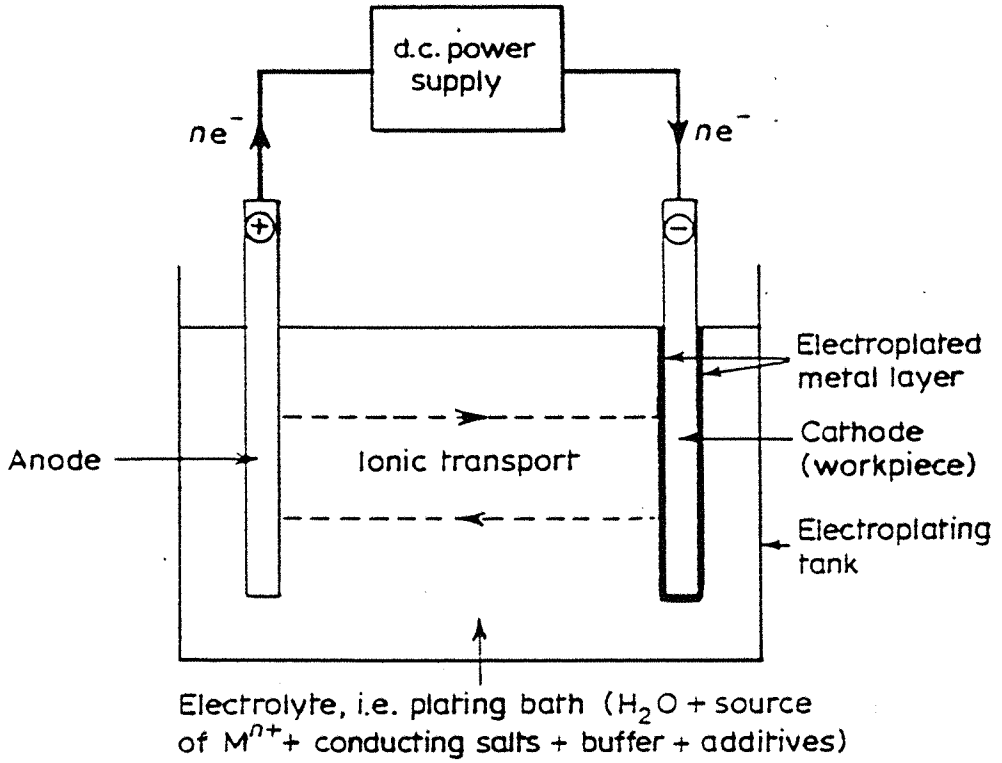

Figure 1.01:Diagram of a typical electroplating bath.

A bath usually includes the following [3];

1) The solution contains the complexed metal to be plated, an inert electrolyte, a buffer and possibly organic additives.
2) The electronically conducting cathode i.e. the workpiece to be plated.
3) The electronically conducting anode which may be soluble or inert.
4) An inert vessel to contain (1) to (3), typically made of steel, rubber-lined steel, polypropylene or polyvinyl chloride.
5) A d.c. electrical power source, typically a regulated transformer or rectifier.

The metal complex chosen should must be reducible within the potential range of the solvent and stable in solution over a wide range of temperature and pH. Generally metal complexes are present in high concentrations (1-3 mol l^{-1}) the

exception being the precious metals (10-30 mmol l^{-1}) due to their cost. The complex usually reduces in a simple electron transfer as shown in equation 1.01, although one or more chemical steps may be involved [3].

$$ML_m^{n+} + ne^- \longrightarrow M + mL \qquad 1.01$$

The inert electrolyte, which may also act as a buffer, increases the conductivity of the solution, minimising the iR drops in the bath which cause differences in the potential over a complex cathode surface. This ensures the rate of deposition is more uniform over whole surface.

A buffer is necessary since the oxygen or water reduction at the workpiece, see equations 1.02 to 1.05 or water oxidation at a non-dissolving anode, see equations 1.06 to 1.07, will alter the local pH. This may lead to the precipitation of metal hydroxides and other species.

$$2H_3O^+ + 2e^- \longrightarrow H_2 + 2H_2O \qquad 1.02$$

$$2H_2O + 2e^- \longrightarrow H_2 + 2OH^- \qquad 1.03$$

$$4H_3O^+ + 4e^- + O_2 \longrightarrow 6H_2O \qquad 1.04$$

$$2H_2O + 4e^- + O_2 \longrightarrow 4OH^- \qquad 1.05$$

$$6H_2O \longrightarrow O_2 + 4H_3O^+ + 4e^- \qquad 1.06$$

$$4OH^- \longrightarrow O_2 + 2H_2O + 4e^- \qquad 1.07$$

Additives are usually low concentration organic molecules and may alter more than one characteristic of the deposit, however, they are conveniently classified as follows [3];

1) Brighteners - For a deposit to be bright, the microscopic roughness of the deposit must be low compared with the wavelength of the incident light so that it is reflected rather than scattered. They usually cause the formation of an even fine grained deposit and, hence, may act by modification of the nucleation process.

2) Levellers - These produce a more level deposit on a macroscopic scale and act by adsorption at points where otherwise there would be rapid deposition of metal. Thus, adsorption of additives occurs preferentially at dislocations because of a higher free energy of adsorption and at peaks because the rate of their diffusion to such points is enhanced; the adsorbed additive will reduce the rate of electron transfer. In practice, many addition agents act as both brighteners and levellers.

3) Structure modifiers - These additives change the structure of the deposit and maybe even the preferred orientation or the type of lattice. Some are used to optimise particular deposit properties and others to adjust the stress in the deposit (stress is due to lattice misfit). The latter are often called "stress relievers".

4) Wetting agents - These are added to accelerate the release of hydrogen gas bubbles from the surface. In their absence, the hydrogen which is often evolved in a parallel reaction to metal deposition can become occluded in the deposit, causing for example, hydrogen embrittlement.

1.1.3. The quality of the deposit

The quality of the deposit depends on the composition of the bath and the electrochemical parameters used for plating e.g. current density. Figure 1.02 shows the normalised current density - voltage curve for a simple reducible complex [3].

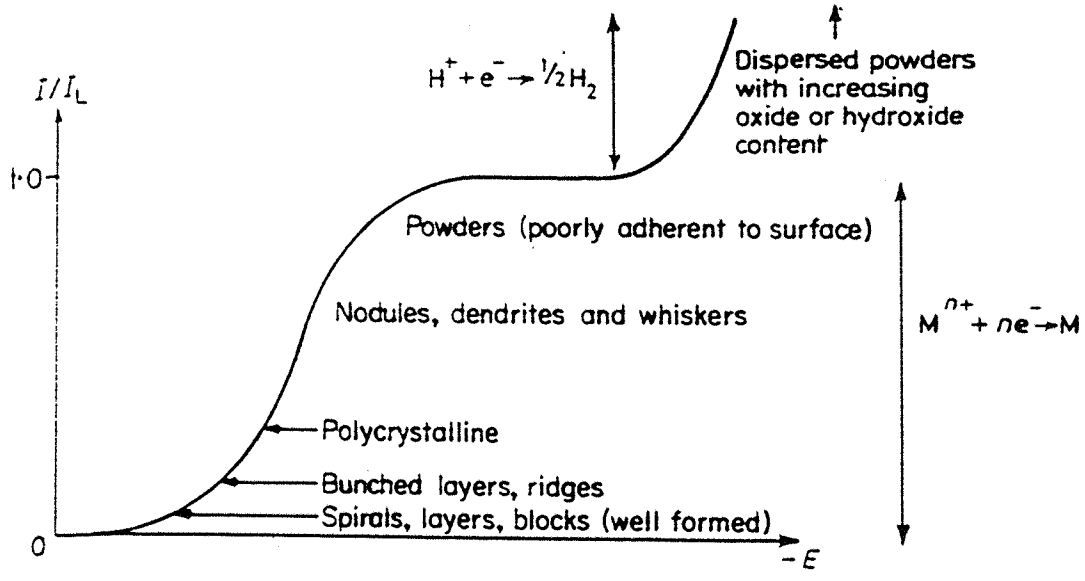

Figure 1.02:Variation in deposit quality with normalised current density.

At low current densities the rate of the surface diffusion of adatoms is fast relative to the rate of electron transfer and so they reach their equilibrium positions in the growing metal lattice. This leads to a compact lattice with well defined microscale fault features e.g. screw dislocations which are observable using electron diffraction. As the current density increases the rate of electron transfer increases whilst the rate of surface diffusion remains constant. Consequently, adatoms have less time to reach the lowest energy positions in the lattice which gives a lower density deposit with coarse macroscale features e.g. the reflectivity decreases as the incident light is scattered rather than reflected. As the current density increases to values where the mass transport of the complex to the cathode is the limiting process, the features become coarser and more frequent until, at the mass transport controlled plateau dendritic growth occurs. Once this form of growth commences, it becomes the only deposition feature due to the enhanced rate of mass transport to the tips of the dendrites (spherical diffusion at the tips is much greater than elsewhere on the

dendrite). The density of the deposit is such that its adhesion to the substrate is significantly affected and loose powders form.

The best deposit is not necessarily formed at low current densities since the composition of the plating bath has an equally important role to play. The best quantitative combination of parameters can only be found empirically.

1.2. Features of the cyclic voltammetry of plating baths

1.2.1. The nucleation overpotential

A feature common in the cyclic voltammograms for the deposition of a metal onto another metal, as takes place in a plating bath, is the nucleation overpotential. This is shown in the cyclic voltammogram in figure 1.03 [4].

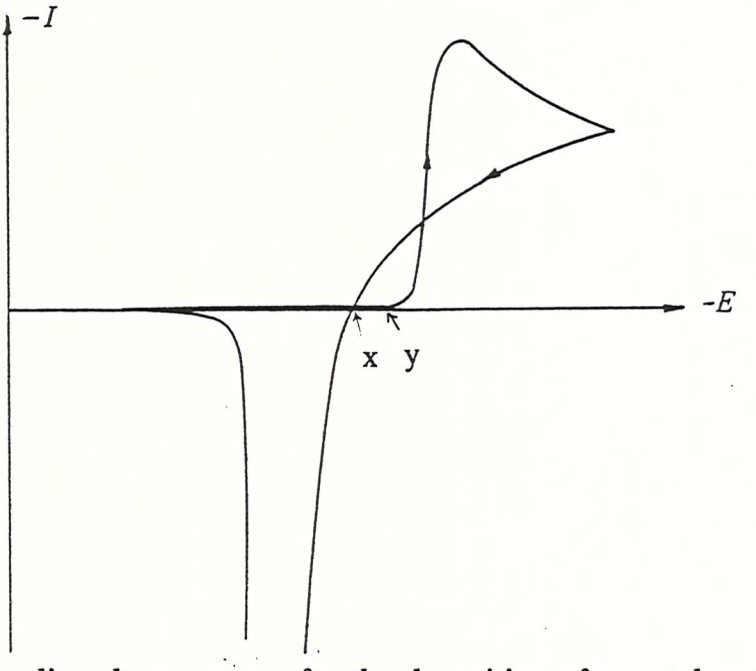

Figure 1.03:The cyclic voltammogram for the deposition of a metal onto a foreign substrate.

The overpotential (y-x) V is necessary to form thermodynamically stable nuclei [2] which will then continue to grow in size provided the potential is more negative than x. Once the potential on the reverse sweep is positive to x deposition stops and the deposited metal may begin to redissolve. The charge passed in generating this sharp symmetrical "stripping" peak is commonly smaller than that passed during deposition proving that not all of the deposited metal has been removed. For fast M/M^{n+} couples x is the equilibrium potential, E_e.

Nuclei can form either instantaneously or progressively and grow in either two or three dimensions. The correct combination can be found by applying a potential step and taking the current-time transient over very short times. At longer times the transients become more difficult to interpret as growing nuclei begin to overlap [4].

Once a few layers have been deposited the electrode acts as a M/M^{n+} electrode which is described in section 1.2.2.

1.2.2. The Tafel region

Once a few layers have been deposited the electrode acts as a M/M^{n+} electrode and the cathodic current is given by equation 1.08.

$$I = I_0 \exp\left(-\frac{\alpha\, n\, F\, \eta}{R\, T}\right) \qquad 1.08$$

where;

I - current density (mA cm^{-2})

I_0- exchange current density (mA cm^{-2})

n - number of electrons involved

F - Faraday constant (96485 C mol^{-1})

R - gas constant (8.314 J K^{-1} mol^{-1})

T - temperature (K)

η - overpotential (V)

α - cathodic electron transfer coefficient

Taking the natural logarithms of equation 1.08 generates equation 1.09.

$$\ln\{I\} = -\frac{\alpha\, n\, F\, \eta}{R\, T} + \ln\{I_0\} \qquad 1.09$$

This linear relationship, valid at high negative overpotentials, is shown in figure 1.04. This enables the values of the cathodic transfer coefficient, α, and the exchange current density, I_0, to be found. The value of α is usually ½. The value of I_0 is the current flowing when the anodic and cathodic currents are equal and opposite at the equilibrium potential i.e. there is no net change in equilibrium concentrations of the reactants and products. Together with the equilibrium potential, E_e, α and I_0 determine the I-E characteristic until mass transport effects begin to play a role.

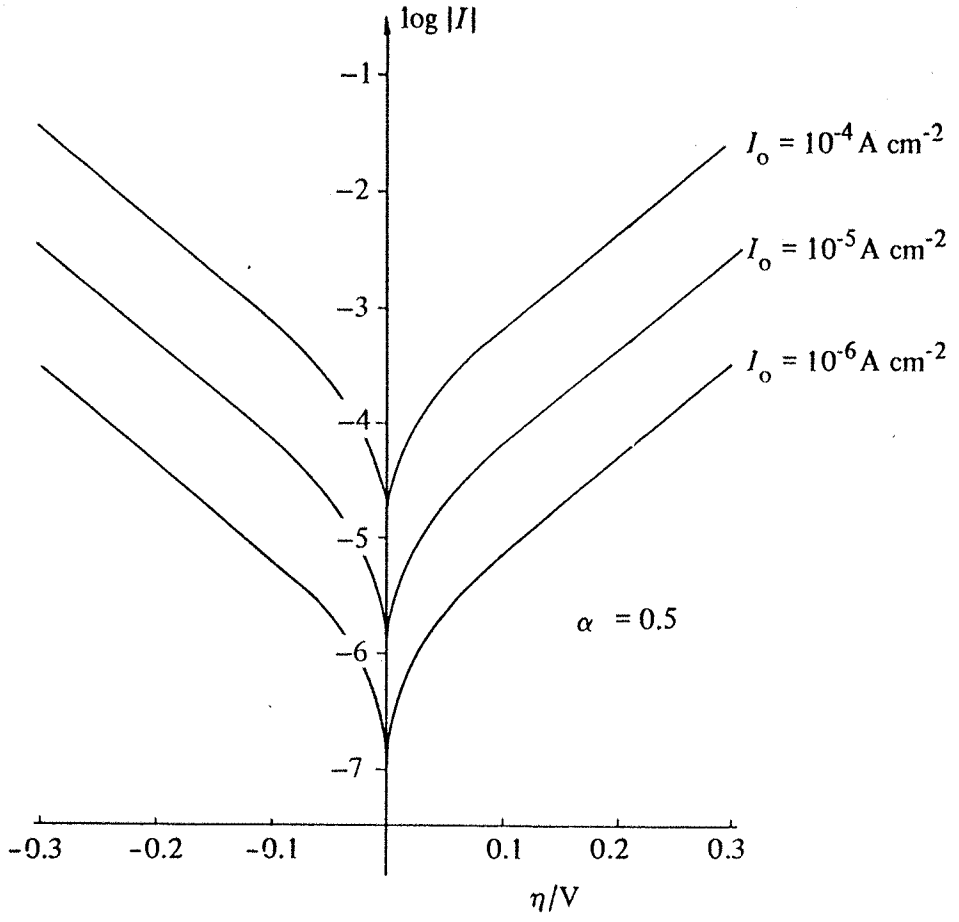

Figure 1.04:Variation of ln I vs η.

1.2.3. Mass transport limitations

At higher overpotentials, the rate of metal deposition is determined by the rate of transport of metal ions to the electrode surface. In general, diffusion, convection and migration can contribute to the mass transport of the electroactive species. The limiting current density, see equation 1.10, is determined by the concentration of the reactant, c, and the mass transport coefficient, k_m, i.e. the mass transport conditions.

$$I_D = n\ F\ k_m\ c \qquad 1.10$$

1.2.4. The influence of the complexing ligand

In the presence of an appropriate ligand, a solvated metal ion, $[MS_m]^{n+}$, will form a complex, see equations 1.11-1.13.

$$MS_m^{n+} + L \rightleftharpoons MS_{m-1}L^{n+} + S \qquad 1.11$$

$$MSL_{m-1}^{n+} + L \rightleftharpoons ML_m^{n+} + S \qquad 1.12$$

$$MS_m^{n+} + mL \rightleftharpoons ML_m^{n+} + mS \qquad 1.13$$

The overall stability constant for complex formation is given by equation 1.14.

$$\beta_m = \frac{[ML_m^{n+}]}{[MS_m^{n+}]\,[L]^m} \qquad 1.14$$

The formation of a complex in solution corresponds to stabilising the metal species in solution and hence the reduction becomes thermodynamically more difficult. Quantitatively, the equilibrium potential for the M^{n+}/M reaction in the absence of ligand is given by equation 1.15.

$$E_e = E_e^\circ + \frac{R\,T}{n\,F} \ln [MS_m^{n+}] \qquad 1.15$$

and in the presence of a ligand by equation 1.16.

$$E_e = \left(E_e^\circ\right)_L + \frac{R\,T}{n\,F} \ln [ML_m^{n+}] \qquad 1.16$$

These equilibrium potentials are equal so equations 1.15 and 1.16 can be combined and equation 1.14 substituted in, to give equation 1.17.

$$\left(E_e^\circ\right)_L - E_e^\circ = -\frac{R\,T}{n\,F} \ln (\beta_m) - \frac{m\,R\,T}{n\,F} \ln [L] \qquad 1.17$$

It can be seen that the shift in the formal potential on the addition of ligand depends on stability constant β_m and the concentration of the free ligand L.

In addition to the thermodynamic effects, the presence of the ligand may also change the kinetics of electron transfer. As a generalisation, the kinetics of electron transfer, correlate with the kinetics of ligand substitution.

1.3. Microelectrodes

1.3.1. Introduction to microelectrodes

A microelectrode is an electrode with at least one dimension small enough that its properties are a function of size [5]. There are several geometries: spherical, hemispherical, disc, ring and line. Figure 1.05 shows these with a planar macroscale electrode and their respective diffusion fields.

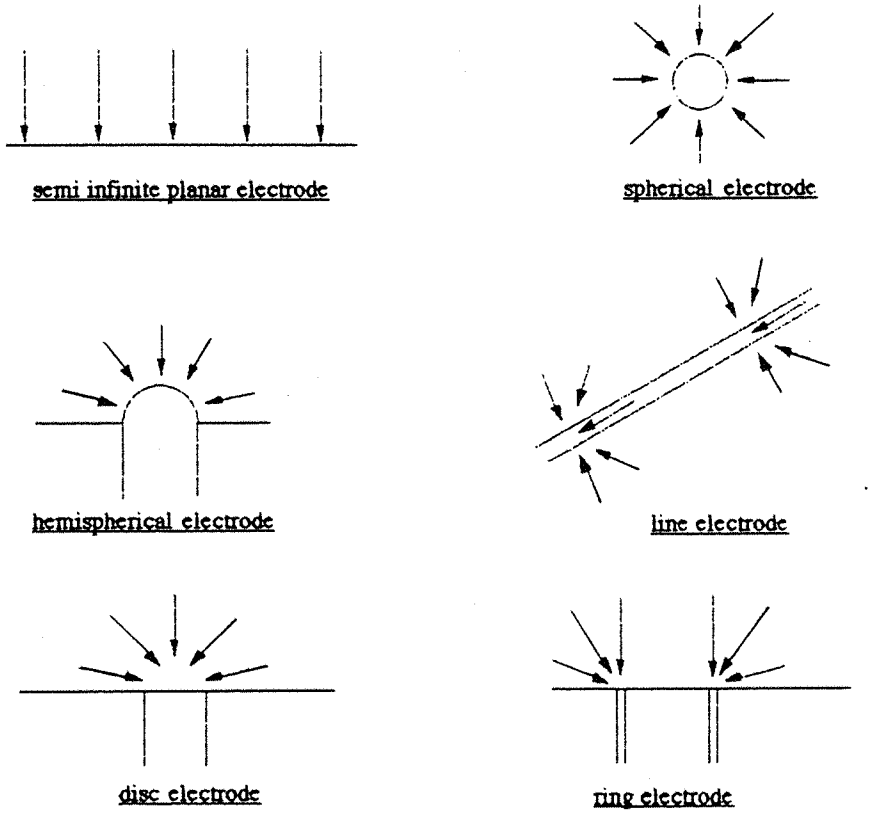

Figure 1.05:A planar macroscale electrode and various microelectrodes with their diffusion fields.

Perfect diffusion fields to microelectrodes are not possible except, in principle, for spherical and hemispherical electrodes. With spherical electrodes, the perfect geometry is broken due to the need for an electrical contact and, in both cases, cleaning of the electrode surface is very difficult. Moreover manufacture of spheres and hemispheres with sufficiently accurate dimensions is extremely difficult and therefore expensive.

Disc, ring and line electrodes may be manufactured and cleaned relatively easily and so they have found wide usage. Of these three, the disc is the commonest. Discs are manufactured from a conducting wire (usually Pt, Au, Ag, W, Cu, C with a radius from 0.1 to 50 μm) surrounded by an insulator (usually glass or epoxy resin with a radius at least five times the radius of the conductor).

1.3.2. The advantages and disadvantages of microelectrodes.

Ideally, the disc is perfectly circular and smooth, but in reality its shape is that of a circle with a fractal perimeter [6,7] whilst its finish depends on the method of polishing and the size of polishing material used. A coarsely polished electrode will present a greater surface area to the solution than a finely polished one, hence the surface finish determines the reproducibility of the results. For this reason, it is important to keep to a constant regime of polishing which ends with a polishing powder with a size much less than the diameter of the electrode. This gives rise to the first of the drawbacks listed below.

1) The active surface area can only be determined with a limited accuracy.
2) The smaller the electrode radius, the more difficult it is to manufacture.
3) The smaller the currents, the more prone signals are to electrical noise.
4) The smaller the microelectrode, the greater its fragility.

The advantages of microelectrodes consistently outweigh the difficulties encountered in using them as publications over the last 10 years have shown [5].

There are two specific advantages [8].

1) The interface between an electrode and electrolyte acts as a capacitor which must be charged whenever the potential is changed. It can be shown [5] that reducing r, reduces the double layer capacitance and the charging time.

Experiments that benefit from this effect include potential step studies of electron transfers with fast coupled chemical reactions [9] and studies of nucleation (where the electrodes small area may limit nucleation to one centre) [6,10,11].

2) Some of the applied potential between two electrodes is always lost in setting up a potential field through the medium in which the current is to flow. This voltage drop is equivalent to the product of cell current i and resistance R and under certain conditions, (high i or R), badly distorts data. Using microelectrodes generates such small currents (nA) that even for highly resistive media (KΩ), the voltage drop (μV)

is negligible. This makes possible electrochemical measurements in solid [12], and gaseous [13] and poorly conducting liquid phases (due to low solvent electrical permittivity or in the absence of electrolyte [9,14-19]).

Alternatively, in systems with high current densities, (A cm^{-2}) the small area of the electrode (10^{-6} cm^2) ensures that only a small current (μA) flows, so reducing the voltage drop. This allows measurements with electroactive species at high concentrations (mol l^{-1}) [20,21] as found in the electrosynthesis and the electroplating industries.

The diffusion field to a disc is not homogenous; it is more concentrated at the perimeter of the circle compared to the centre. This is accounted for by a correction factor to the current density of a spherical electrode, since this electrode's current density is the simplest to calculate [4].

For reaction 1.18 the current density at a spherical electrode is given by equation 1.19.

$$O + ne^- = R \qquad 1.18$$

$$I = n\,F\,c\left(\frac{D_o}{\pi\,t}\right)^{\frac{1}{2}} + n\,F\,c\left(\frac{D_o}{r_s}\right) \qquad 1.19$$

where:

I - current density (mA cm^{-2})

n - the number of electrons involved

F - Faraday constant (96485 C mol^{-1})

D_O- diffusion coefficient of O (cm^2 s^{-1})

c - concentration (mol cm^{-3})

t - time (s)

r_s- radius of spherical electrode (cm)

There are two possible limiting forms for this equation [2];

(a) When $t \rightarrow 0$ the current density is given by equation 1.20.

$$I = \frac{n\ F\ c\ D_O^{1/2}}{\pi^{1/2}\ t^{1/2}} \qquad 1.20$$

This is the Cottrell equation which describes linear diffusion of species O to a planar macro scale electrode.

(b) When $t \rightarrow \infty$ the current density is given by equation 1.21.

$$I = \frac{n\ F\ c\ D_o}{r_s} \qquad 1.21$$

This is the steady state equation for diffusion of species O to a spherical microelectrode.

Experimentally, "intermediate" times are avoided since results are difficult to interpret. The change from "intermediate" to "long" or "short" term behaviour depends on the surface area of the electrode [5].

The correction factor due to the increased current density at the edges of the disc (radius r) is given by equation 1.22 [22].

$$r_s = \frac{\pi r}{4} \qquad 1.22$$

Substituting equation 1.22 into equation 1.21 gives equation 1.23.

$$I = \frac{4\ n\ F\ D_O\ c}{\pi\ r} \qquad 1.23$$

This high rate of steady state diffusion means that microelectrodes are independent of convection and can be used to monitor flowing streams with variable flow rates.

1.4. Platinum

1.4.1. Introduction

Platinum is often found in ores which also contain ruthenium, osmium, rhodium, iridium and palladium; it is for this reason that these 6 metals have become known as the platinum group metals. Significant deposits of these ores have been found in Russia, South Africa and Canada. They require an involved extraction procedure to separate the chemically similar metals. World production of these 6 metals was 200 tonnes in 1984 with 45% being platinum [23].

Platinum is a dense, high melting point metal, although at its position in the periodic table, both densities and melting points are dropping. Rhodium, iridium, palladium and platinum have the face centred cubic structure predicted by band theory for nearly filled d orbitals. It is the most ductile metal after gold and silver and can easily be worked into thin sheets [24].

The main physical properties of platinum are shown in table 1.01 [23,24].

Property	Value for platinum
Atomic number	70
Atomic mass (g mol^{-1})	195.09
Electronic configuration	[Xe] $4f^{14}$ $5d^{9}$ $6s^{1}$
Crystal structure	Face centred cubic
Density (g cm^{-3} at 293 K)	21.45
Melting point (K)	2046.5
Boiling point (K estimated)	4803
Thermal conductivity (J cm^{-1} cm^{-2} s^{-1} K^{-1})	0.71
Linear coefficient of expansion (K^{-1})	8.9×10^{-6}
Electrical resistance (Ω cm^{-1} at 293 K)	10.6×10^{-6}
Youngs modulus, annealed (tonne cm^{-2})	1.7×10^{3}

Table 1.01 :The main physical properties of platinum.

The coefficient of expansion is very similar to that of soda glass and for several years platinum was fused into glass items where a permanent seal over a large temperature range was required, e.g. light bulbs. It has now been superseded by a much cheaper Cu/Ni/Fe alloy. A much commoner use of the metal today is as a catalyst, e.g. oxidation of NH_3 to HNO_3 [25] and of organic vapours from car exhausts. Platinum is extremely resistant to corrosion by acids and oxygen, only dissolving in aqua regia and not oxidising in air at any temperature. Both water and jet engine turbine blades are coated with platinum, as is apparatus used for handling hot hydrogen fluoride and other corrosive chemicals. Platinum is also used in the jewellery industry being prized for rarity and appearance. Its Youngs modulus value is greater than that of gold but it is usually alloyed with a small amount of palladium to further increase its hardness [24].

1.4.2. Oxidation states

Oxidation states V and VI are rare, being limited to 6 co-ordinate fluoro complexes [26]. Oxidation states I and III are also rare since they leave unpaired d electrons in the outer orbitals, however, if these are stabilised by M-M bonding an oxidation state of I or III may occur. Many compounds previously thought to be Pt^{III} are actually mixed valence compounds containing Pt^{II} and Pt^{IV} [23].

The oxidation states II and IV are the most common and are usually square planar and octahedrally co-ordinated respectively, however, some Pt^{II} compounds are known to be 5 co-ordinate.

Platinum also has a significant number of compounds in which it shows an oxidation state of zero. The co-ordination numbers for these compounds may be 2, 3, or 4 although only ligands which can accept significant π back donation of electron density will stabilise this oxidation state.

1.4.3. Hard and soft acids and bases

The distinction of hard and soft acids and bases are an interpretation [27] of the trends of stabilities in metal complexes [28]. There is a gradual change from hard to soft behaviour for both acids and bases, but they are normally categorised into one of 3 groups; hard, soft or borderline. Generally hard acids and bases are small slightly polarisable species whilst soft acids and bases are larger and more polarisable. Pearson reported that hard acids prefer to bind to hard bases and soft acids prefer to bind to soft bases.

The theoretical basis of these empirical observations is probably due to several factors, each contributing to a varying extent under different conditions.

In classifying aqueous transition metal complexes as hard or soft, it is necessary to realise that borderline hard/soft metal ions will be influenced by the hardness or softness of the ligands already present in the complex. Fortunately, Pt^{2+} with its d^8 configuration is definitely a soft acid whilst the ligands H_2O, OH^- and NH_3, all have small slightly polarisable atoms through which bonding occurs and therefore are classified as hard bases [29].

This is not to say that aqueous hydroxy or ammine platinum complexes do not exist but that soft acids prefer soft bases. Soft acids will bind to hard bases in the absence of anything softer, and bind to a weaker hard base if given a choice. The real strengths of hard and soft species can be measured using $pK_a(H_3O^+)$ and $pK_a(CH_3Hg^+(H_2O))$ respectively [30]; a strong hard or soft acid is one with a low pK_a and a strong hard or soft base is one with a high pK_a. Hence a soft acid already bound to a hard base will preferentially bind to a soft base, see equation 1.24.

$$[PtCl_4]^{2-} \xrightarrow{I^-} [PtCl_3I]^{2-} \xrightarrow{I^-} [PtCl_2I_2]^{2-} \xrightarrow{I^-} [PtClI_3]^{2-} \xrightarrow{I^-} [PtI_4]^{2-} \quad 1.24$$

It is for this reason that preparation of bis(ammine)dichloroplatinum(II) from the tetrachloroplatinate(II) anion with ammonia is always contaminated with a small amount of potassium tetrakis(ammine)platinum(II) tetrachloroplatinate(II), Magnus' green salt [31,32], see equation 1.25.

$$[PtCl_4]^{2-} \xrightarrow{NH_3} [PtCl_3(NH_3)]^{-} \xrightarrow{NH_3} [PtCl_2(NH_3)_2] \xrightarrow{NH_3}$$

$$[PtCl(NH_3)_3]^{+} \xrightarrow{NH_3} [Pt(NH_3)_4]^{2+} \qquad 1.25$$

The weak hard base, ammonia, replaces the strong hard base, chloride, in bonding to the strong soft acid, platinum. This is so thermodynamically favourable that, to some extent, the ligand substitution reaction continues to form the tri and tetrakis ammine substituted platinum complex.

The different intermediate geometries are not mentioned here as they cannot be explained on the basis of the thermodynamics of the platinum-ligand bond strengths. They can, however, be explained by kinetic effects described in the section 1.4.4. Thus, it should noted that the concept of hard and soft acids and bases cannot alone explain all the observed ligand substitutions of platinum, see equation 1.26 in section 1.4.4.

1.4.4. The trans effect and influence

The trans effect has been defined [33,34] as "the effect of a co-ordinated group on the rate of substitution reactions of ligands opposite to it in a metal complex" i.e. the trans effect is a transition state effect. The trans influence describes the ability of a ligand trans to a second ligand to lengthen or weaken the second ligand's bond to the metal i.e. the trans influence is a ground state effect.

An approximate order of the decreasing labilising ability [29,34] is;

$C_2H_4 \approx Me_2COH.CC.HOCMe_2 \approx NO \approx CO \approx CN^- > R_3Sb > R_3P > R_3As \approx H^- \approx SC(NH_2)_2 > CH_3^- > C_6H_5^- > SCN^- > NO_2^- > I^- > Br^- > Cl^- > NH_3 > OH^- > H_2O$

The high position of the pure σ bonding ligands, such as H^- and CH_3^-, means that σ bonding as well as π bonding needs to be taken into account.

Altering the trans ligand can raise the rate of reaction by 10^4 [35] and the relative positions of different ligands in the complex can dictate the products of ligand substitution reactions, see equation 1.26 and 1.27.

$$[PtI_4]^{2-} \xrightarrow{NH_3} [PtI_3(NH_3)]^- \xrightarrow{NH_3} cis\text{-}[PtI_2(NH_3)_2] \qquad 1.26$$

$$[Pt(NH_3)_4]^{2+} \xrightarrow{I^-} [Pt(NH_3)_3I]^+ \xrightarrow{I^-} trans\text{-}[Pt(NH_3)I_2] \qquad 1.27$$

Generally, the effect of ligands cis to the leaving group only have a small effect relative to the trans effect on the rate of reaction. If, however, the leaving group and its trans ligand have approximately the same trans directing strength then the cis effect can be 10^4 times more important than the trans [34].

1.4.5. Ligand substitution mechanisms

Platinum(II) square planar complexes are kinetically inert, i.e. they have extremely low rates of ligand substitution which make them very convenient to study. This has generated a large amount of literature [32,40-46] which is impossible to cover here, rather the mechanism for a specific set of conditions will be considered.

The general mechanism for a complex $[ML_4]$ attacked by a nucleophile Y in a polar co-ordinating solvent S is a combination of two reactions as figure 1.06 shows.

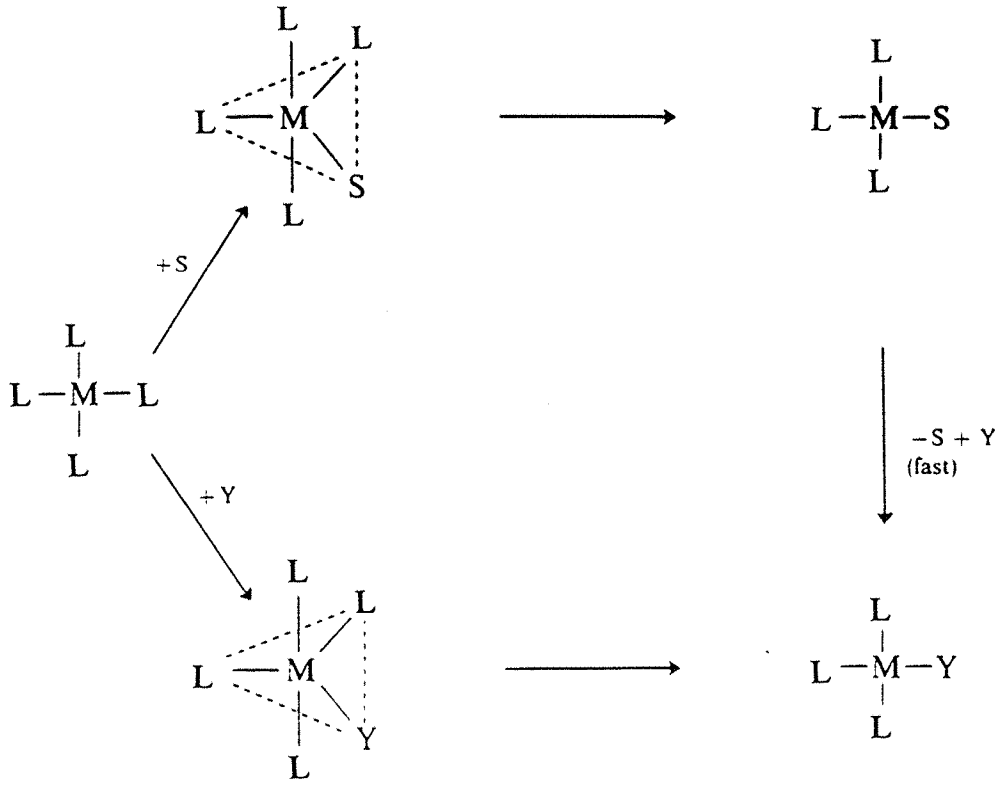

Figure 1.06:Reaction scheme for the ligand substitution of ML_n by the nucleophile Y in the polar co-ordinating solvent S.

For this reaction mechanism the two term rate equation is given by equations 1.28 and 1.29. If the only nucleophile present is the solvent, S, then the rate equation is given by equation 1.30.

$$Rate = (k_2[S] + k_2[Y])[ML_4] \qquad 1.28$$

$$= (k_1' + k_2[Y])[ML_4] \qquad 1.29$$

$$= k_1'[ML_4] \qquad 1.30$$

At least 3 reaction profiles, shown in figure 1.07, fit this mechanism [34]. It has been suggested [43] that reaction profile (b) exists for S > L in the trans effect series and (c) for S < L. Thus, for S = H_2O and L = NH_3 reaction profile (c) would be expected.

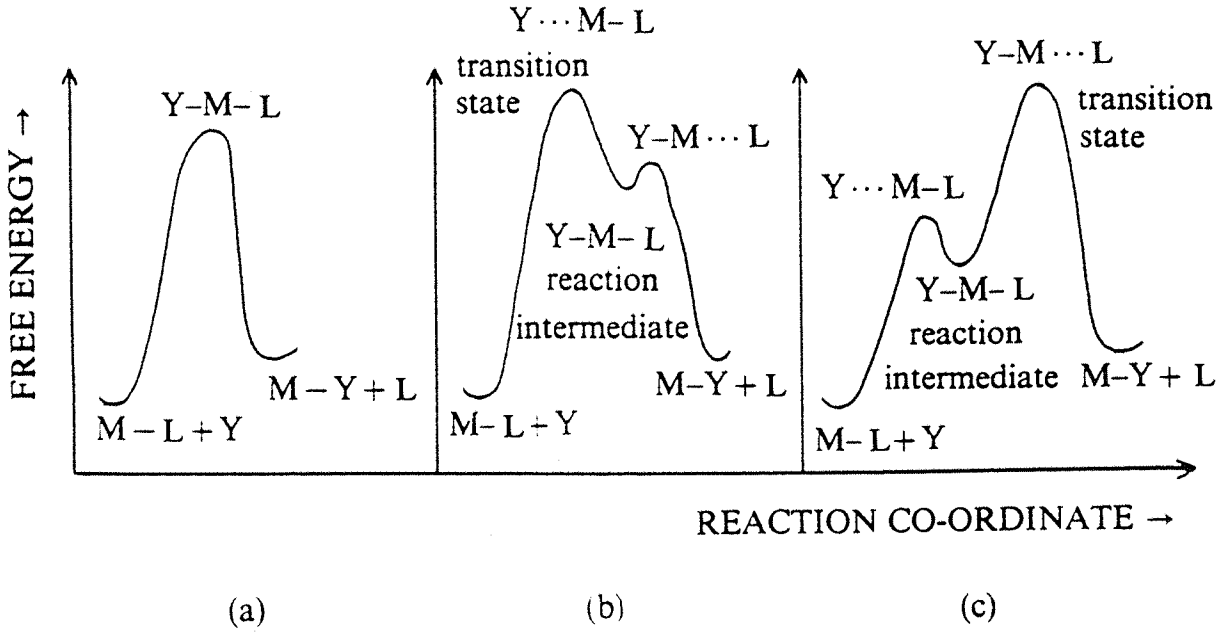

Figure 1.07:Three possible reaction profiles for nucleophilic substitution of the complex ML_n by solvent S.

1.4.6. Platinum nuclear magnetic resonance spectroscopy

Platinum has several naturally occurring isotopes only one of which has a nuclear spin. Table 1.02 tabulates all the naturally occurring isotopes of platinum with their abundances and other nuclear data [36,37].

Isotope	Natural abundance (%)	Type of radioactive decay (if any) and half life (years)	Nuclear spin quantum number	Magnetogyric ratio (10^7 rad s^{-1} T^{-1})
^{191}Pt	0.02	α emitter, 10^{12}	0	0
^{192}Pt	0.78	α emitter, 10^{15}	0	0
^{194}Pt	32.9	none	0	0
^{195}Pt	33.8	none	½	5.8383
^{196}Pt	25.8	none	0	0
^{198}Pt	7.2	none	0	0

Table 1.02 :The natural abundance and nuclear properties of the isotopes of platinum.

Thus, approximately one third of naturally occurring platinum will give a signal in nuclear magnetic resonance spectroscopy.

The compound chosen for referencing any NMR chemical shifts needs to have several properties [38];

1) It should be readily available.
2) It should be stable in solution.
3) It should resonate over a narrow frequency range.
4) It should appear at either the high or low field end of the frequency range.

The reference, found by the experience of the majority of users, to be the most convenient, is aqueous $[PtCl_6]^{2-}$. This complex is readily available, stable in solution and resonates towards the low field end of the frequency range. It can, however, be split into five peaks due to the two different isotopes of naturally occurring chlorine. When it is taken into account that the chemical shift range for ^{195}Pt NMR

spectroscopy is greater than 13000 ppm [39] (compared to that for ^1H of 70 ppm, including transition metal hydrides) the first of these problems becomes insignificant. Its only real drawback is its large temperature dependence (0.84 ppm K^{-1}).

The large variation in chemical shift is due to the changing chemical environment of the platinum complex in solution which alters the effective magnetic field experienced by the platinum nucleus. The chemical shift depends mainly on the ligands bound to the nucleus, although other physical factors which can affect the chemical shift are mentioned first [38].

1) Solvent - the chemical shift of identical platinum complexes changes with solvent, see table 1.03.

Solvent	Complex	Chemical shift (ppm)
H_2O	$Na_2[PtCl_4]$	-1614
CH_3OH	$Na_2[PtCl_4]$	-1477
CH_2Cl_2	$(Bu_4N)_2[PtCl_4]$	-1416
CH_3CN	$(Bu_4N)_2[PtCl_4]$	-1388
$(CH_3)_2CO$	$(Bu_4N)_2[PtCl_4]$	-1384
$(CH_3)_2SO$	$(Bu_4N)_2[PtCl_4]$	-1372

Table 1.03 :Variation in the platinum chemical shift (relative to $[PtCl_6]^{2-}$) on changing solvent.

Thus, the assignment of peaks in different spectra must be made in the same solvent since changing the solvent may shift the peaks by up to 300 ppm.

2) Temperature - the chemical shift of platinum complexes varies with temperature, see table 1.04 [37].

Thus, assignment of peaks in different spectra at two different temperatures can be made since a change in temperature usually leads to a change in chemical shift of a few ppm.

Complex	Change in chemical shift with temperature (ppm K^{-1})
$[PtCl_6]^{2-}$	0.84
trans-$[PtBr_2(PPr^n_3)_2]$	0.33
trans-$[PtHCl(PPr^n_3)_2]$	0.1

Table 1.04 :Variation in the platinum chemical shift with temperature.

Coordinating ligands have empirically been found to effect the chemical shift in the following ways [38];

1) For related complexes, as the ligands trans influence increases the resonance moves to a lower frequency i.e. a more negative chemical shift, see table 1.05.

Complex	Chemical shift (ppm)
$[PtCl_3(H_2O)]^-$	-1180
$[PtCl_3(NMe_3)]^-$	-1715
$[PtCl_3(PMe_3)]^-$	-3500

Table 1.05 :Variation of chemical shift (relative to $[PtCl_6]^{2-}$) with trans influence.

The trans influence series decreases in the order P > N > O whilst the chemical shifts for these complexes becomes increasingly positive.

2) Chemical shifts are little influenced by substituents on the donor atoms but do vary with the geometric isomer present, see table 1.06.

$[PtCl_2(PR_3)_2]$ chemical shift (ppm)		$[PtBr_2(SMe_2)_2]$ chemical shift (ppm)	
Cis isomer	Trans isomer	Cis isomer	Trans isomer
x	x+500	-3879	-3899

Table 1.06 :Variation of chemical shift (reference $[PtCl_6]^{2-}$) with geometric isomer.

3) For related complexes as a ligand group is descended the resonance often but not always, moves to a lower frequency i.e. to a more negative chemical shift, see table 1.07.

Chemical shift for $[PtCl(SMe_2)_2X]$ (ppm)		
X = Cl	X = Br	X = I
-3424	-3666	-5131

Table 1.07 :Variation of chemical shift (relative to $[PtCl_6]^{2-}$) on descending a ligand group.

If the ligands surrounding the platinum also have a nuclear spin then fine structure will be present in the spectrum. In this study nitrogen and oxygen ligands have been used. Table 1.08 tabulates all the naturally occurring isotopes of these two elements with their abundances and other nuclear data [36,37].

Isotope	Natural abundance (%)	Type of radioactive decay (if any) and half life(years)	Nuclear spin quantum number	Magnetogyric ratio (10^7 rad s^{-1} T^{-1})
^{14}N	99.6	none	1	+1.9338
^{15}N	0.4	none	½	-2.7126
^{16}O	99.76	none	0	0
^{17}O	0.04	none	2½	-3.6280
^{18}O	0.20	none	0	0

Table 1.08 :The natural abundance and nuclear properties of the isotopes of nitrogen and oxygen.

It can be seen from the table that the natural occurrence of ^{17}O is so low that no splitting can be detected. The natural occurrence of ^{15}N is larger and splitting due to this isomer could be seen if it were not swamped by the signal from ^{14}N.

The first order spectrum of n nuclei, nuclear spin I, coupling to one platinum

nucleus, nuclear spin ½, will give a spectrum with (2 n I + 1) peaks. These peaks will be of different intensities which can easily be found using variants of Pascals triangle. The sum of (2 I + 1) nearest neighbours in the n^{th} row, above each element to be calculated in the $(n+1)^{th}$ row, gives the value for that element. The $(n+1)^{th}$ row gives the intensities for n nuclei coupling to one platinum nucleus [37].

e.g. $[Pt(NH_3)_4]^{2+}$

This complex has 9 (2.4.1 + 1) peaks, the intensities of which are given by

number of nuclei coupling	triangle variant	number of row
0	1	1
1	1 1 1	2
2	1 2 3 2 1	3
3	1 3 6 7 6 3 1	4
4	1 4 10 16 19 16 10 4 1	5

The peaks in this example, rather than being distinct from each other and so giving a well defined coupling constant, are broad giving an inaccurate value of the coupling constant. This is because all nuclei with I > ½ have a quadrupolar moment as well as nuclear magnetic moment which alters the relaxation time of the ^{14}N relative to that of the ^{195}Pt. The source of the problem is that the relaxation of the quadrupolar nucleus is neither fast enough to totally decouple from the platinum nor slow enough to fully couple to the platinum. The broad resonances can be sharpened by thermal decoupling i.e. heating the sample, since the quadrupolar effect is temperature dependant. Alternatively, if ^{15}N (I = ½) enriched compounds are used in the preparation of the complex there is no quadrupolar moment and no line broadening. For this reason, most of the platinum - nitrogen coupling constants obtained are for ^{15}N complexes. These coupling constants may be compared to ^{14}N complexes by multiplying by 0.714, the ratio of the ^{14}N and ^{15}N magnetogyric ratios.

The value of the coupling constant varies with [38];

1) The oxidation state of the metal

e.g. cis-$[PtCl_2(^{15}N(CH_2)_{11}CH_3)_2]$	$^1J(^{195}Pt\text{-}^{15}N$ trans to Cl)	351 Hz
cis-$[PtCl_4(^{15}N(CH_2)_{11}CH_3)_2]$	$^1J(^{195}Pt\text{-}^{15}N$ trans to Cl)	249 Hz

2) The geometry of the ligands

e.g. $[Pt(H_2O)(^{15}NH_3)_3]^{2+}$	$^1J(^{195}Pt\text{-}^{15}N$ trans to $H_2O)$	376 Hz
	$^1J(^{195}Pt\text{-}^{15}N$ trans to $^{15}NH_3)$	299 Hz

3) The trans influence of the ligands

e.g. $[Pt(^{15}NH_3)_3I]^+$	$^1J(^{195}Pt\text{-}^{15}N$ trans to I)	289 Hz
$[Pt(^{15}NH_3)_3Br]^+$	$^1J(^{195}Pt\text{-}^{15}N$ trans to Br)	319 Hz
$[Pt(^{15}NH_3)_3Cl]^+$	$^1J(^{195}Pt\text{-}^{15}N$ trans to Cl)	331 Hz

From this summary it can be seen that both the chemical shift, δ, and the one bond coupling constant, ^1J, can be used to help identify the platinum complexes in the plating bath.

1.4.7. Platinum electroplating

Although the first patent for platinum deposition was dated 1837 [47], the deposits obtained were unsuitable for any applications. Investigations into deposition mechanisms led to refinements of the chloride based electrolytes until in 1931 when $[Pt(NH_3)_2(NO_2)_2]$, subsequently named the platinum P salt, was first used for electroplating. This complex, in its original bath composition, has several disadvantages;

1) It shows a jump in current efficiency of 60% at 333 K.
2) It is unstable and may form a non electroactive platinum complex with time.
3) It cannot deposit thick layers of platinum without cracking.

Various baths based on this complex have been developed but none with current efficiency greater than 40%. Despite this it is still the most popular complex in use today, although others have been developed, see table 1.08.

Recently Johnson Matthey have introduced a new plating bath, the Pt5Q bath, based on the tetrakis(ammine)platinum(II) cation in a low concentration phosphate buffer at pH 10. It is capable of depositing thick layers of platinum but must be operated at temperatures above 363 K.

Fundamental studies of platinum electroplating systems are very limited [47] although there have been descriptions of the polarography of platinum complexes [48,49]. Very recently, Le Penven [50] has reported a preliminary study of the Pt5Q bath and this thesis is an extension of that work.

Composition	Conc. ($g\ l^{-1}$)	Temp. (°C)	Current density ($A\ dm^{-2}$)	Current efficiency (%)	[Ref]
$H_2[PtCl_6]$ HCl	10- 50 180-300	45- 90	2.5 - 3.5	15 - 20	51
$(NH_4)_2[PtCl_6]$ $Na_3C_6H_5O_7.2H_2O$ NH_4Cl	15 100 4- 5	80- 90	0.5 - 1.0	70	52
$[Pt(NH_3)_2(NO_2)_2]$ NH_3 NH_4NO_3 $NaNO_2$	8- 16.5 50 100 10	90- 95	0.3 - 2.0	10	53
$[Pt(NH_3)_2(NO_2)_2]$ HBF_4 $NaBF_4$	20 50-100 80-120	70- 90	2.0 - 5.0	14 - 18	54
$[Pt(NH_3)_2(NO_2)_2]$ NH_2SO_3H	6- 20 20-100	65-100	0.2 - 2.0	15	55
$[Pt(NH_3)_2(NO_2)_2]$ H_3PO_4	8 80	75-100	0.5 - 3.0	15	56
$[Pt(NH_3)_2(NO_2)_2]$ H_3PO_4 H_2SO_4	6- 20 10-100 10-100	75-100	0.5 - 3.0	15	57
$[Pt(NH_3)_2(NO_2)_2]$ CH_3COONa Na_2CO_3	16.5 70 100	80- 90	0.5	35 - 40	52
$H_2[Pt(NH_3)_2SO_4]$ H_2SO_4	10 pH 2	30- 70	2.5	10 - 15	58
$Na_2[Pt(OH)_6].2H_2O$ NaOH	20 10	75	0.8	100	59
$Na_2[Pt(OH)_6].2H_2O$ NaOH $Na_2C_2O_4$ Na_2SO_4	18.5 5.1 5.1 30.8	65- 80	0.8	80	60
$H_2[Pt(OH)_6]$ KOH	20 15	75	0.75	100	61
$K_2[Pt(OH)_6]$ K_2SO_4	20 15	70- 90	0.3 - 1.0	10 - 50	61
$[PtCl_4].5H_2O$ NH_4Cl $(NH_4)_2HPO_4$ Na_2HPO_4	7.5 20- 25 20 100	70- 90	0.3 - 1.0	10 - 50	62

Table 1.08 :Established platinum electroplating baths.

2. EXPERIMENTAL

2.1. Electrochemical equipment

Potentiostats and waveform generators were both supplied by HI-TEK, models DT2101 and PPRI respectively. Currents from microelectrode experiments were amplified by an in-house current follower which converted currents in the range 1 x 10^{-4} to 1 x 10^{-8} A to a 10 V output signal.

Constant current supplies were taken from two sources;

1) a purpose built transformer made by Farnell, model L30B

2) a potentiostat with a high wattage resistor across the working and reference electrodes.

The latter arrangement was more stable to voltage spikes from the mains supply and was preferred.

Current-voltage curves were displayed on a X-Y recorder from Gould, 60000 series.

The oil bath used in all electrochemical experiments was manufactured by Memmert, model MO200. Liquid paraffin was used as the oil over the temperature range 304 K to 391 K which gave cell temperatures of 303 K to 372 K.

All the potentials quoted are versus a Ag/AgCl (in saturated KCl) reference electrode from Radiometer (model K801) which has a reference potential of +0.204 V compared to the Standard Hydrogen Electrode at 293 K [63]. The pH was measured using a combination glass and Ag/AgCl (in saturated KCl) reference electrode from Radiometer (model GK2401B) attached to a Data Scientific pH meter, model PTI-15. Silver/silver chloride electrodes were preferred due to their stability with respect to high temperatures (up to 373 K). Calibration of the pH meter was made using buffer solutions (prepared in the laboratory using GPR reagents) of 1.38, 6.85, 9.18 and 11.72 [63].

2.2.1. Microelectrode experiments

The cell used was conical in shape, see figure 2.01, with a volume of 70 cm^3 although typically volumes of 20 cm^3 of solution were used.

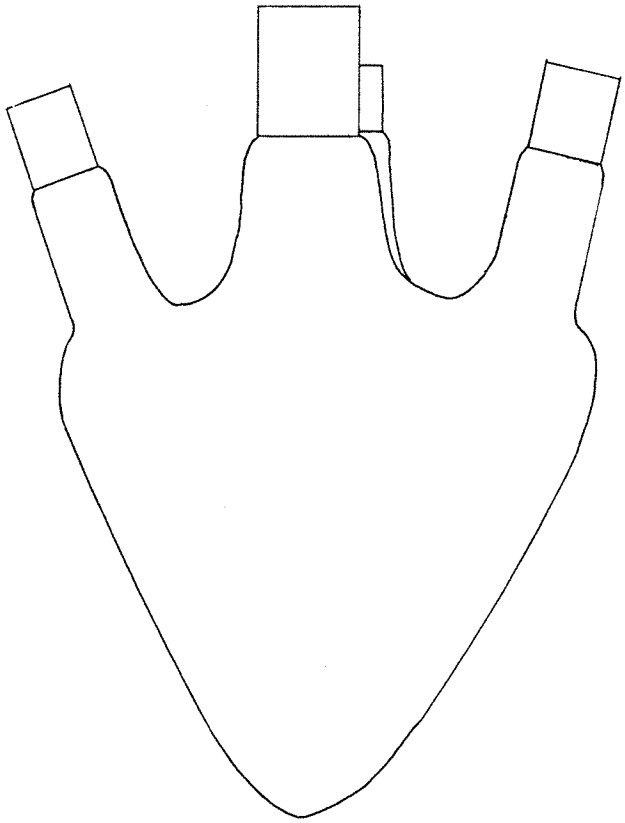

Figure 2.01:Diagram of the cell used in the microelectrode experiments.

Microdiscs of various radii (2.5, 5, 12.5, 25 μm) were prepared from platinum wire (Goodfellow Metals Limited) which was soldered to a thicker nickel wire and the assembly sealed in a glass capillary (1.5 mm), see figure 2.02.

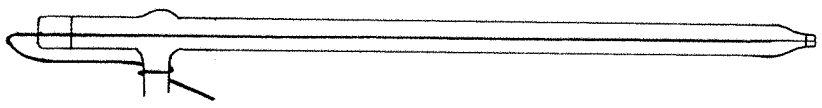

Figure 2.02:Diagram of the microdisc electrode used in the microelectrode experiments.

The microdiscs surface was polished before each cyclic voltammogram with 5, 1, 0.3 and 0.05 μm alumina (Buehler Ltd) on the polishing cloth, Microcloth (Buehler Ltd). The tip of the electrode was rinsed with deionised water between each polish and after the final polish it was cleaned by ultrasound in deionised water for approximately 20 s.

Periodically, the radii of the electrodes were checked using a freshly prepared solution of potassium ferricyanide (GPR, 5 mmol l^{-1}) in a solution of potassium chloride electrolyte (GPR, 1 mol l^{-1}) [64]. The potential was swept from +0.7 to -0.2 V (at decreasing scan rates for increasing radius of the electrode) and the limiting current for the reduction of Fe^{III} to Fe^{II} was measured. Using equation 2.01 and the appropriate value of D for $[Fe(CN)_6]^{3-}$ the radii of the microdiscs, on which all the current densities in chapter 3 depend, were calculated.

$$i = 4\,n\,F\,D\,c\,r \qquad 2.01$$

where

i - current (A)

n - number of electrons involved (1)

F - Faraday constant (96485 C mol^{-1})

D - Diffusion coefficient for $[Fe(CN)_6]^{3-}$ (6.3×10^{-6} cm^2 s^{-1} [64])

c - concentration (mol cm^{-3})

r - radius (cm)

The solution of the platinum (II) salt under study was heated to the appropriate temperature and a pH reading taken. The solution was then deoxygenated with a stream of nitrogen pre-heated to the temperature of the solution by passing it through a copper coil immersed in the same oil bath. With care the temperature change on deoxygenation could be kept to ± 1 K. In the cell the nitrogen passed through a glass sinter (grade 3) to enhance deoxygenation. Electrodes were dipped in the solution 2 minutes before the experiment was started.

Due to the small currents passed by microelectrodes, a two electrode configuration could be used with the reference electrode also acting as the secondary electrode. The circuit, see figure 2.03, was connected just prior to the voltage ramp being applied.

All cyclic voltammograms were then recorded at 25 mV s^{-1} for a freshly polished platinum microdisc (r=12.5 μm) although for different solutions, potential limits, temperatures and pHs were varied.

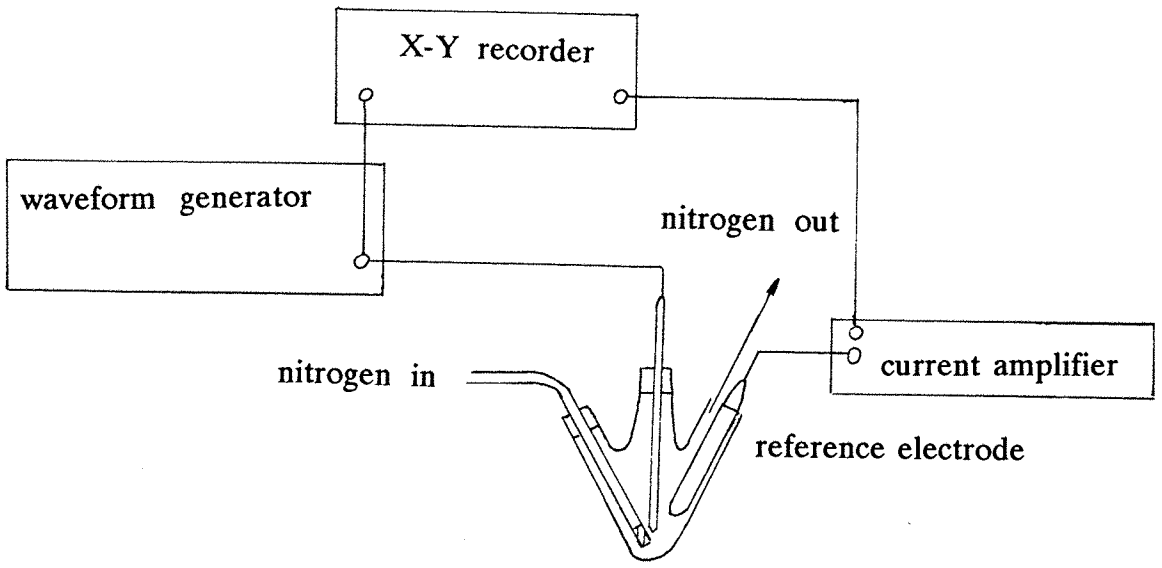

Figure 2.03:Circuit diagram for the microelectrode experiments.

2.2.2. Macroelectrode experiments

The cell, see figure 2.04, has a volume of 140 cm^3 although typically volumes of solution of 100 cm^3 were used.

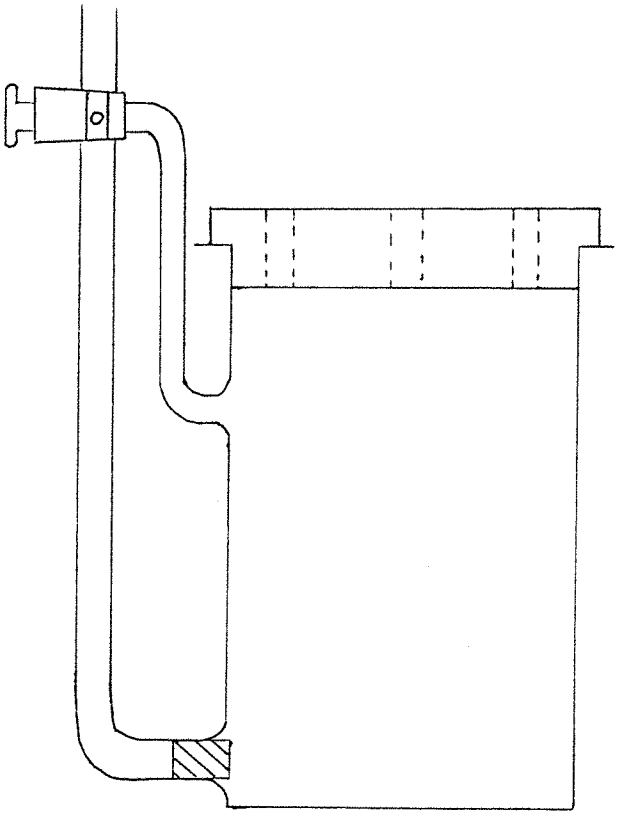

Figure 2.04:The cell used for macroscale platinum deposition experiments.

Copper panels (laboratory manufactured, 25 mm x 25 mm × 0.057 mm) were degreased with CH_2Cl_2 (GPR), cleaned in H_2SO_4 (GPR, 1 mol l^{-1}) and rinsed in H_2O (Millipore system). In each of these three solutions the panel was subjected to approximately 2 minutes of ultrasound which was followed by physically wiping the panel with a tissue impregnated with the solution and finally rinsing the panel in deionised water.

The panel was then dried, a closed sprung loop of copper wire fixed to it, in order to make an electrical contact and it was then weighed. The panel was attached to the circuit and dipped into the solution between the two anodes 1-2 minutes (depending on the temperature of the solution) before the circuit was connected. A

lid was placed on the cell to prevent excessive evaporation and the nitrogen, previously passing through the solution, was directed over it. The current was switched on and the deposition started.

The constant current, -i, was drawn from the reference electrode terminal of a potentiostat which was connected to the working electrode by a resistor (2.2 Ω, 7 W), see figure 2.05 [4]. The deposition current, -i, is given by Ohms law (-Voltage/Resistance). The two anodes were connected as normal.

After deposition the panel was removed, rinsed in deionised water, dried and reweighed. From the increase in mass and the charge passed, the current efficiency can be calculated, see section 3.2.3.

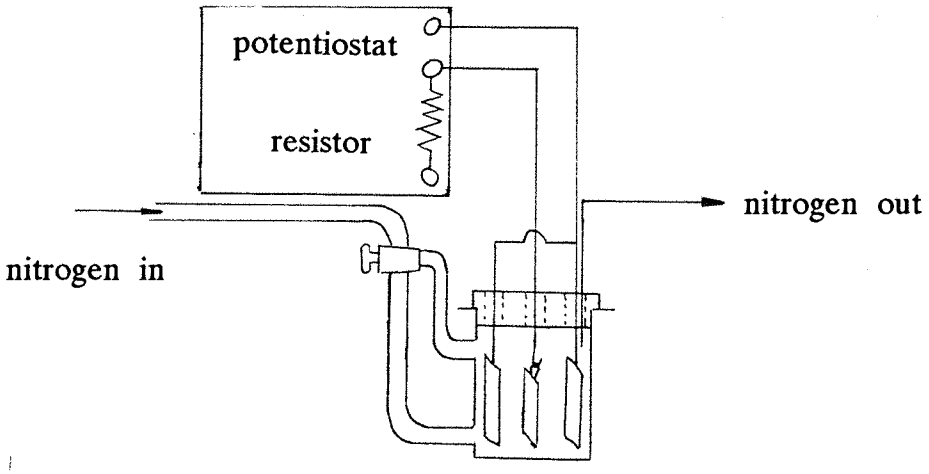

Figure 2.05:Circuit diagram for the electroplating experiments.

2.3. Spectrometers

Ultra violet - visible spectra were recorded on a Perkin Elmer lambda 19 UV/VIS/NIR spectrophotometer using 1 cm path length quartz cells over the range 200 to 1000 nm.

Infrared spectra were recorded on a Perkin Elmer 1710 FTIR spectrophotometer using caesium iodide cells with nujol as the solvent. The range scanned was from 400 to 4400 cm^{-1}. Potassium bromide discs were not used as the bromide might bond to the platinum compound in the disc generating false peaks.

Nuclear magnetic resonance spectra of the isotope ^{195}Pt were recorded on a Bruker AM360 spectrometer using 10 mm borosilicate glass tubes. The aqueous solutions contained deuterium oxide ($\approx$ 5 % v/v) to provide the lock. All chemical shifts are relative to an external reference of the aqueous hexachloroplatinate(IV) anion and are given positive values to lower shielding.

Atomic absorbtion spectra were recorded on a Perkin Elmer 2380 atomic absorbtion spectrophotometer using an air/acetylene (fuel lean i.e. oxidising flame) at λ = 265.9 nm with a slit of 0.7 nm. Lanthanum (III) chloride heptahydrate (AAS grade, 0.2% w/w) was added to eliminate the chemical interference effects of the high concentrations of perchlorate and chloride ions (from the sample and standard solutions respectively). An alternative method to eliminate interferences is to increase the temperature of the flame by using an acetylene/nitrous oxide mixture This, however, decreases the sensitivity of the technique.

The concentration of platinum in solution was obtained by the reverse extrapolation of a line formed by five points from the method of standard additions.

2.4. Preparations

2.4.1. $[Pt(NH_3)_4]HPO_4$

This compound was supplied by Johnson Matthey as a solution containing tetrakis(ammine)platinum(II) hydrogen orthophosphate (5 g l^{-1} Pt) in a buffer of di-sodium hydrogen orthophosphate dodecahydrate (10.1 g l^{-1}) at pH 10.1 and is more commonly known in the electroplating industry as the Pt5Q solution.

It was prepared by Johnson Matthey by dissolving the white powder, $[Pt(NH_3)_4](HCO_3)_2$ (25.6 mmol, 9.86g) in an orthophosphoric acid solution to evolve the carbon dioxide. The solution is then adjusted to pH $\approx$10.1 with NaOH (56.1 mmol l^{-1}, 2.25 g) where the dihydrogen orthophosphate is deprotonated to hydrogen orthophosphate.

$$[Pt(NH_3)_4](HCO_3)_2 + H_3PO_4 = [Pt(NH_3)_4]HPO_4 + 2H_2O + 2CO_2\uparrow \qquad 2.02$$

2.4.2. $[Pt(H_2O)_4](ClO_4)_2$

Two methods of preparation were attempted. The method described here is based on Elding's preparation using silver [65] and was successful if followed closely. Another novel approach was unsuccessful and is reported in section 3.2.1.

Potassium tetrachloroplatinate(II), $K_2[PtCl_4]$, (5 mmol, 2.08 g) was dissolved in perchloric acid, $HClO_4$, (1 mol l^{-1}, 200 cm^3) making the solution 25 mmol l^{-1} in platinum. At 293 K a white crystalline precipitate of potassium perchlorate, $KClO_4$, appeared in the dark red solution, see equation 2.03. This dissolved as the aluminum foil covered conical flask (500 cm^3) containing the stirred solution was heated to 343 K using an oil bath.

$$K_2[PtCl_4] + 2ClO_4^- = [PtCl_4]^{2-} + 2KClO_4\downarrow \qquad 2.03$$

Silver perchlorate monohydrate, $AgClO_4.H_2O$, (20 mmol, 4.51 g) was dissolved in $HClO_4$ (1 mol l^{-1}, 225 cm^3) making the solution 89 mmol l^{-1} in silver. Aliquots of this solution were added to the aqueous platinum complex every 30 minutes followed by deoxygenation of the solution for 2 minutes. Between additions, nitrogen was passed over the solution. As shown by Elding, it was important to carefully control the ratio of [Pt]:[Ag] to prevent precipitation of the insoluble $Ag_2[PtCl_4]$. When all the silver had been added nitrogen was left slowly passing over the solution for 14 hours and thereafter the solution was left with a positive pressure of nitrogen over it at 343 K for 7 days.

$$[PtCl_4]^{2-} + 4Ag^+ \xrightarrow{H_2O} [Pt(H_2O)_4]^{2+} + 4AgCl\downarrow \qquad 2.04$$

The light brown precipitate of AgCl, see equation 2.04, was vacuum filtered off from the hot solution (> 333 K to ensure no $KClO_4$ precipitated in the sinter) to leave a clear, yellow filtrate of $[Pt(H_2O)_4](ClO_4)_2$. The AgCl was washed with $HClO_4$ (1 mol l^{-1}, 65 cm^3, 333 K) and dried in vacuo over silica gel for at least 7 hours to determine the extent of reaction. The actual yield was 2.87 g, 20 mmol equivalent to 100 % yield. The washings were added to the filtrate and the solution left to cool to 293 K. No white precipitate appeared due to the increased volume of solution being able to dissolve all the $KClO_4$ present at 293 K.

2.4.3. cis-$[Pt(NH_3)_2(H_2O)_2](ClO_4)_2$

This synthesis described here is based on the preparation of cis platin, $[Pt(NH_3)_2Cl_2]$, described by Dhara [66]. It avoids contamination of the product by tetrakis(ammine)platinum(II) tetrachloroplatinate(II), commonly known as Magnus green salt.

Potassium tetrachloroplatinate(II), $K_2[PtCl_4]$, (1.5 mmol, 0.62 g) was dissolved in water (50 cm^3) to form a clear red solution. Ten minutes after adding a ten-fold excess of potassium iodide [67], KI, (60 mmol, 9.96 g) in water (10 cm^3) at 293 K, the stirred solution turned an opaque dark brown. Its pH was adjusted to 10 using aqueous NaOH (10% w/w) and it was heated at 353 K for 5 minutes. These conditions ensured that most of the tetrachloroplatinate(II) was converted to tetraiodoplatinate(II), see equation 2.05.

$$[PtCl_4]^{2-} + 4I^- = [PtI_4]^{2-} + 4Cl^- \qquad 2.05$$

Ammonium chloride, NH_4Cl, (3 mmol, 0.161 g) was dissolved in aqueous sodium hydroxide (3 mmol, 6 cm^3 of 0.5 mol l^{-1}). This fresh solution of aqueous ammonium hydroxide, NH_4OH, (3 mmol) was added to the tetraiodoplatinate(II) at 353 K, the heating stopped and the flask loosely stoppered (to prevent ammonia escaping). A deep yellow precipitate of cis-$[PtI_2(NH_3)_2]$ began to appear after 2 minutes and the cooling solution was left stirring for 12 hours, see equation 2.06.

$$[PtI_4]^{2-} + 2NH_3(aq) = [PtI_2(NH_3)_2]\downarrow + 2I^- \qquad 2.06$$

The precipitate was filtered off of the clear orange solution washed with water (2 x 50 cm^3, 313 K), and dried in vacuo over silica gel for at least 6 hours. The actual yield was 0.670 g, 1.39 mmol equivalent to 93 % of the theoretical yield.

The cis-$[PtI_2(NH_3)_2]$ (1.39 mmol, 0.67 g) formed a suspension when added to $HClO_4$ (1 mol l^{-1}, 100 cm^3). This stirred suspension was heated to 353 K and silver perchlorate monohydrate, $AgClO_4.H_2O$, (2.78 mmol, 0.626 g) in $HClO_4$ (1 mol l^{-1}, 25 cm^3) was added. The solution started to clear and a yellow precipitate began to form in the bottom of the flask. Heating was stopped 30 minutes after the addition of the silver and the reaction stirred for a further 12 hours, see equation 2.07.

$$[PtI_2(NH_3)_2] + 2Ag^+ = [Pt(NH_3)_2(H_2O)_2]^{2+} + 2AgI\downarrow \qquad 2.07$$

The light green precipitate of AgI was filtered, washed with $HClO_4$ (1 mol l^{-1}, 20 cm^3) and dried in vacuo over silica gel for at least 6 hours. The actual yield was 0.648 g, 2.76 mmol equivalent to 99% of the theoretical yield.

The washings were added to the filtrate to give a solution of cis-$[Pt(NH_3)_2(H_2O)_2](ClO_4)_2$ (10 mmol l^{-1}) in $HClO_4$ (1 mol l^{-1}).

3. RESULTS AND DISCUSSION

3.1. Introduction

The objective of this study was to further the understanding of the chemistry of the Pt5Q plating bath and to investigate platinum deposition from related solutions. In this way, it was hoped to improve the performance of this important new bath. Johnson Matthey have already taken out patents [68] and the bath is in use commercially for electroplating large components. Its main advantage over other platinum electroplating systems being the rapid deposition of thick, low-stress layers.

The solution contains

$[Pt(NH_3)_4]HPO_4$	25.6 mmol l^{-1}
$Na_2HPO_4.12H_2O$	28.2 mmol l^{-1}
with a pH of	10-10.6

The temperature of operation, above 363 K, has been reported to be essential to obtaining high current efficiencies for platinum deposition; below this temperature the current efficiency drops rapidly to $\approx$10% [50,68]. This elevated temperature is particularly inconvenient, requiring pre-heating of large workpieces before plating.

Developments of the Pt5Q plating bath were sought that would reduce this high operating temperature, enabling easier operation.

3.2. $[Pt(NH_3)_4]^{2+}$ solution

3.2.1. Preparation and characterisation of the solution

A solution of $[Pt(NH_3)_4]HPO_4$ (25.6 mmol l^{-1}) containing the buffer Na_2HPO_4 (28.1 mmol l^{-1}) at pH 10.1 was supplied by Johnson Matthey. It was prepared by dissolving $[Pt(NH_3)_4](HCO_3)_2$, a white powder also available from Johnson Matthey, in orthophosphoric acid, to evolve the carbon dioxide, and then adjusting the pH to ≈10.1 with NaOH (56.2 mmol l^{-1}).

It was already known [50] that the Pt5Q solution gave only 1 peak in a low resolution ^{195}Pt NMR at δ=-2575 ppm (relative to $[PtCl_6]^{2-}$). The resolution could be improved by increasing the number of scans collected and continuously irradiating at the proton resonance frequency to eliminate any ^1H coupling.

Figure 3.01 shows a high resolution ^{195}Pt $\{^1H\}$ NMR spectrum of the $[Pt(NH_3)_4]^{2+}$ after taking ≈70000 scans over ≈30 hours at 300 K.

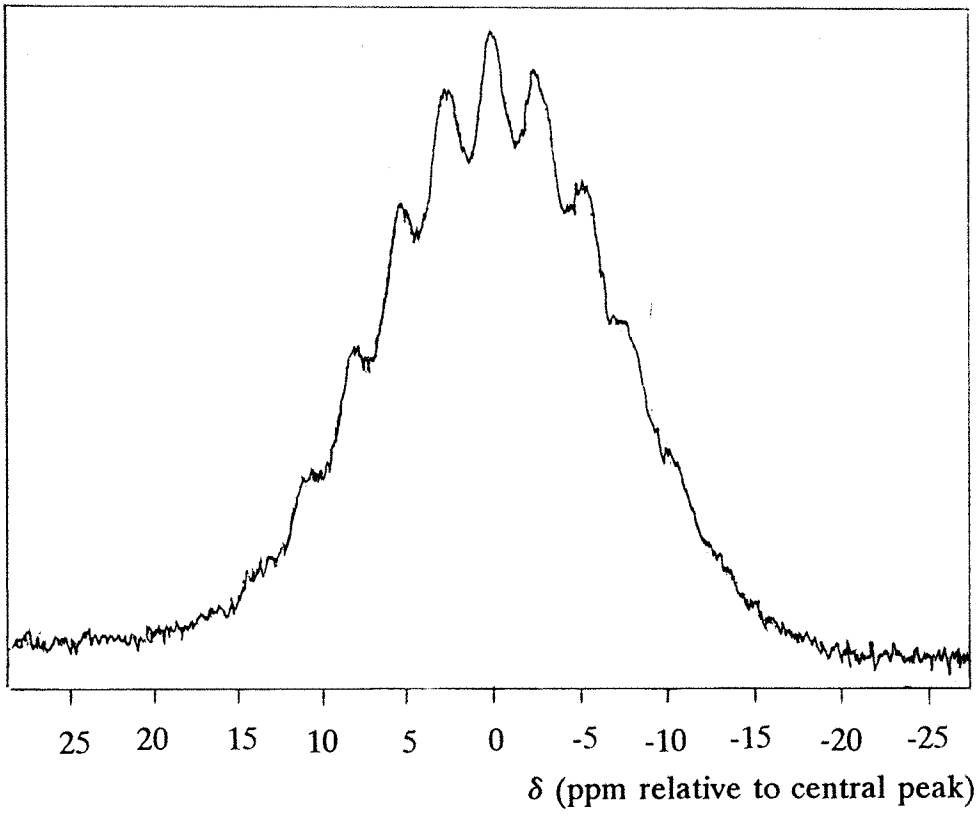

Figure 3.01: ^{195}Pt $\{^1H\}$ NMR spectrum of $[Pt(NH_3)_4]^{2+}$ (25.6 mmol l^{-1}) in Na_2HPO_4 (28.1 mmol l^{-1}) at pH 10 and 300 K after ≈70000 scans at 77.2 MHz δ=-2568 ppm (reference $[PtCl_6]^{2-}$)

It can be seen that this higher resolution spectrum has fine structure in which nine lines are discernable. These are the nine lines expected form a simple first order spectra of 4 nuclei, nuclear spin 1, coupling to another spin nucleus, nuclear spin ½. The intensity of such a nonet of lines should be 1:4:10:16:19:16:10:4:1 and this was reflected qualitatively in the spectrum obtained. The chemical shift, δ, for the central line was -2568 ppm, whilst the 1 bond coupling constant, $^{1}J(^{195}Pt\text{-}^{14}N)$, was 202 ± 5 Hz. Literature values of the chemical shift were -2580 ppm for $[Pt(^{15}NH_3)_4]^{2+}$ [69,70] and -2575 ppm for $[Pt(^{14}NH_3)_4]^{2+}$ [50] confirming the presence of the tetrakis(ammine)platinum(II) cation. No literature values could be found for the $^{195}Pt\text{-}^{14}N$ coupling constant, $^{1}J(^{195}Pt\text{-}^{14}N)$, but the literature value of $^{1}J(^{195}Pt\text{-}^{15}N)$ (for $[Pt(NH_3)_4]^{2+}$) has been reported to be 284 and 287 Hz [69,70]. A comparison of $^{1}J(^{195}Pt\text{-}^{15}N)$ can be made to that of $^{1}J(^{195}Pt\text{-}^{14}N)$ by multiplying $^{1}J(^{195}Pt\text{-}^{15}N)$ by the ratio of the ^{14}N:^{15}N magnetogyric constants, 0.714. This gives a literature value of 205 Hz for $^{1}J(^{195}Pt\text{-}^{14}N)$ which compares well to the experimentally determined value of 202 Hz and further confirms the presence of $[Pt(NH_3)_4]^{2+}$ in solution.

A low resolution ^{195}Pt NMR study of the Pt5Q solution at various temperatures has already been reported [50]. It was found that only one peak (δ=-2576 ppm relative to $[PtCl_6]^{2-}$) was detectable at all temperatures and that this peak shifted only 0.32 ppm K^{-1}. From this it was concluded that the tetrakis(ammine)platinum(II) cation was the only major platinum species in the Pt5Q solution at all temperatures.

3.2.2. Microelectrode studies of platinum deposition from tetrakis(ammine)platinum(II) hydrogen orthophosphate

A solution of $[Pt(NH_3)_4]HPO_4$ (25.6 mmol l^{-1}) and $Na_2HPO_4.12H_2O$ (28.1 mmol l^{-1}), initial pH 10.1, was heated at the selected temperature for 60 minutes. A further pH reading was taken and then the pH adjusted to 10.4 with aqueous NaOH (2.5 mol l^{-1}). The solution was then deoxygenated with a stream of N_2, pre-heated to the temperature of the solution by passing it through a copper coil immersed in the same oil bath. It was important to avoid contact of both the Pt5Q solution and the N_2 with organic materials; even routing the N_2 through plastic tubing seemed to inhibit platinum deposition.

Cyclic voltammograms were then recorded between 0 and -1 V (vs Ag/AgCl in saturated KCl) at 25 mV s^{-1} for a freshly polished platinum microdisc (r=12.5 μm) at 20 minute intervals. After 7 voltammograms had been collected another pH reading was taken. Fresh Pt5Q solution (20 cm^3) was used for each temperature.

Figure 3.02 shows the both the forward and reverse scans of a cyclic voltammogram at 368 K.

On the forward scan of this cyclic voltammogram, the current density positive of -0.6 V is low, $<$-1 mA cm^{-2}, but at potentials negative of this value, it increases rapidly until reaching a maximum of I_p(forward)=-30 mA cm^{-2} at E_p(forward)=-0.74 V . It then rapidly decreases to a minimum of $<$-5 mA cm^{-2} at -0.86 V before increasing again due to water reduction commencing on the freshly deposited platinum.

On the reverse scan a cathodic peak is also observed at E_p(reverse)=-0.74 V, I_p(reverse)=-41 mA cm^{-2}. At potentials positive of -0.60 V the current density has decreased to $<$-1 mA cm^{-2}.

The cyclic voltammogram of the phosphate buffer with no tetrakis(ammine)platinum(II) hydrogen orthophosphate present shows no peaks prior to hydrogen evolution at -0.95 V. Hence, the peaks at -0.74 V on both the forward and reverse scans were due to an electroactive Pt(II) complex reducing to Pt(0) at the microdisc.

The increased size of the reverse peak was due to platinum which deposited on

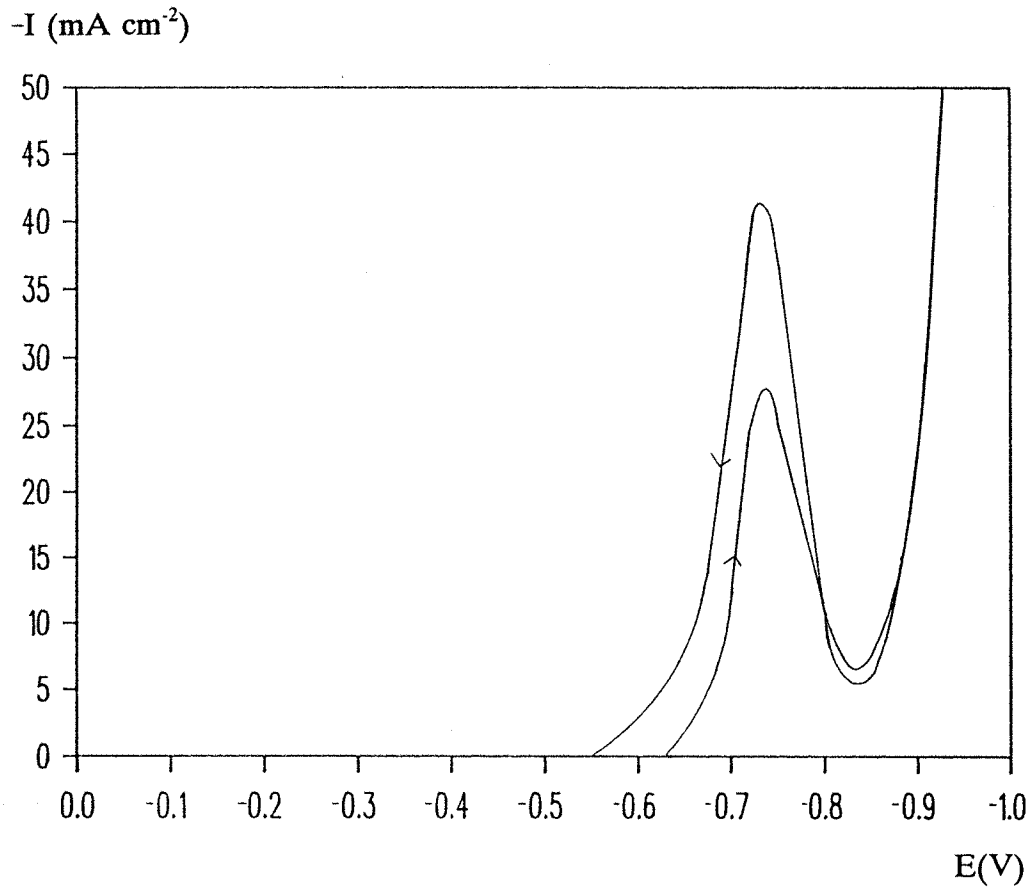

Figure 3.02:I-E curve using a Pt microdisc (r=12.5 μm) scanned from 0 to -1 V (vs Ag/AgCl in saturated KCl) at 25 mV s^{-1} in a deoxygenated solution containing $[Pt(NH_3)_4]^{2+}$ (25.6 mmol l^{-1}) at pH 10.4 and 368 K.

the forward scan, either increasing the surface area or activity of the electrode. The presence of peaks, rather than waves, was attributed to another reaction blocking platinum deposition at potentials between E_p and the start of hydrogen evolution. This reaction must be highly reversible since both forward and reverse scans are affected in the same way to approximately the same extent. An absorbed species blocking platinum reduction is the most likely explanation, the H atom has already been suggested as the adsorbed species [50].

Table 3.01 tabulates the values for both I_p(forward and reverse) at 20 minute intervals and the mean of selected values at all the temperatures studied.

The main points illustrated by table 3.01 are;

1) There is no trend of either I_p(forward) or I_p(reverse) with time, at a constant temperature. Thus, these microelectrode experiments, show that the concentration of the electroactive complex in solution does not change with time at constant temperature.

2) The peak current densities obtained from repeated experiments were not completely reproducible. The data from the reverse scans were certainly more reproducible than those from the forward scans. Moreover, most peak current densities at one temperature fell within a reasonable range but there were some rogue data. It was therefore decided to ignore the "bad runs" when calculating the mean peak current densities at each temperature. It is believed that the poor reproducibility was associated with the surface preparation of the microdisc.

3) I_p(forward and reverse) increased rapidly with increasing temperature, see figure 3.03. The variation is far larger than the uncertainty resulting from the reproducibility problem discussed in (2). Below 343 K, the forward scan showed no discernable signal. The reverse scan still showed a small peak but this too was absent at 293 K.

The appearance of a reduction peak at elevated temperatures only suggests that the electroactive complex is formed in a slow chemical step from $[Pt(NH_3)_4]^{2+}$. Figure 3.03 shows the typical reverse scans at 4 different temperatures.

It can be seen that E_p did not vary significantly with temperature showing that only one electroactive complex was present at all temperatures. I_p(reverse) depends so strongly on temperature, see figure 3.04, that an increase in the diffusion coefficient alone cannot be responsible. This suggests that the rate of formation of the electroactive complex must be increasing with temperature.

Figure 3.05 (a) shows a plot of ln $\{I_p$(reverse mean)$\}$ vs T^{-1}.

It can be seen that this Arrhenius plot is reasonably linear allowing the energy of activation to be estimated from the slope. Its value was 116 kJ mol^{-1}. This high value is indicative of a chemical step producing a complex which is actually reduced in the electron transfer step.

The expected variation of the diffusion controlled current density, I_D, for a 25.6 mmol l^{-1} solution of a Pt(II) electroactive complex at a platinum microdisc electrode ($r=12.5$ μm) with temperature can be estimated using equations 3.01 and 3.02.

T (K)	scan	$-I_p$ (mA cm^{-2}) x minutes after pH adjustment							mean of underlined I_p values (mA cm^{-2})
		20 min	40 min	60 min	80 min	100 min	120 min	140 min	
343	for	0	0	0	0	0	0	0	0
	rev	3	2	2	2	1	1	1	2
348	for	0	3	0	0	0	0	2	1
	rev	5	5	4	4	3	3	3	4
353	for	7	9	1	1	1	2	6	7
	rev	9	9	8	8	1	8	9	9
358	for	8	2	11	13	9	11	9	10
	rev	18	13	14	15	14	13	13	14
363	for	15	15	6	16	10	2	2	14
	rev	24	23	23	27	23	18	20	23
368	for	34	27	18	30	31	32	17	31
	rev	39	35	37	41	43	43	39	40
372	for	51	28	29	*	23	7	10	27
	rev	54	41	51	*	49	37	40	45

* The microelectrode broke and was replaced with another of the same radius.

Table 3.01 :Variation of I_p(forward and reverse) with time as a function of temperature for a platinum microdisc (r=12.5 μm) scanned from 0 to -1 V (vs Ag/AgCl in saturated KCl) at 25 mV s^{-1} in Pt5Q solution at pH 10.2-10.4

$$I_D = 4\ n\ F\ D_T\ c\ r \qquad 3.01$$

$$D_T = D_{293}\exp -\frac{E_A}{R}\left(\frac{1}{T} - \frac{1}{293}\right) \qquad 3.02$$

where:

n - number of electrons involved in reduction (2)

F - Faraday constant (96485 C mol^{-1})

T - temperature (K)

D_T- diffusion coefficient at temperature T ($cm^2\ s^{-1}$)

c - concentration of the electroactive complex (mol cm^{-3})

r - radius of the microdisc (cm)

E_A- activation energy (kJ mol^{-1})

R - gas constant (8.314 J K^{-1} mol^{-1})

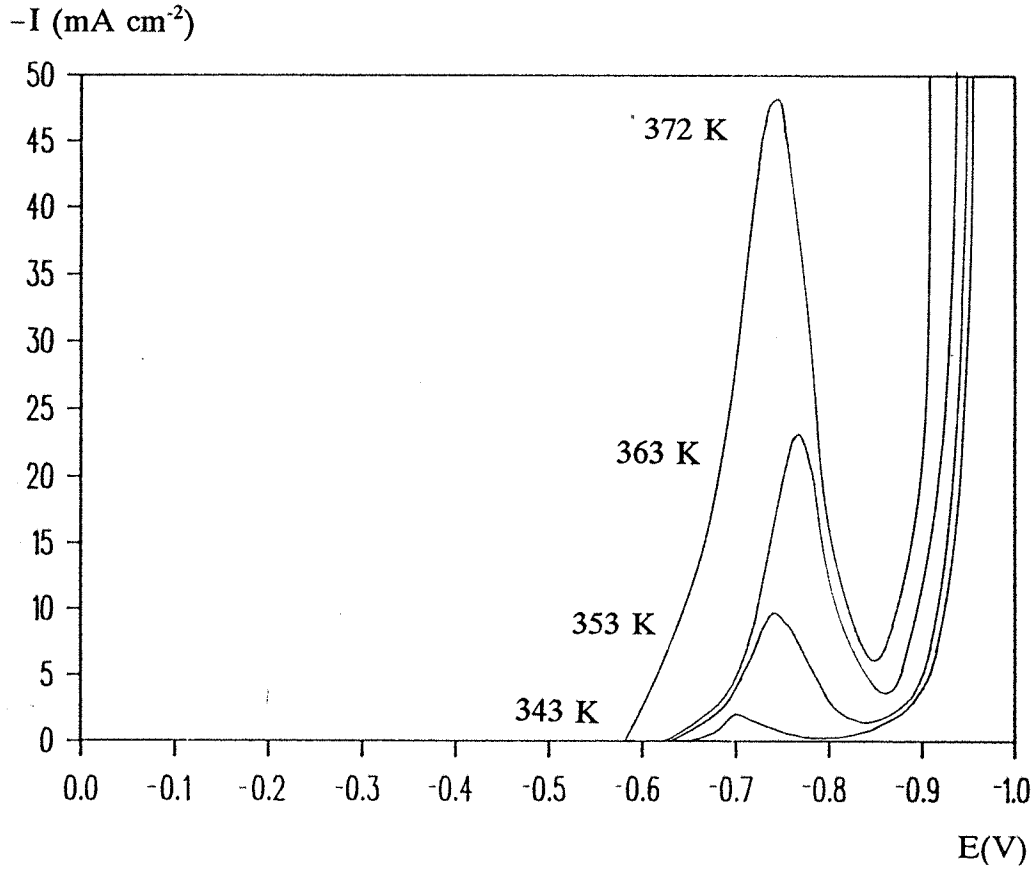

Figure 3.03 :I-E curves (reverse scans) using a Pt microdisc (r=12.5 μm) scanned from 0 to -1 V (vs Ag/AgCl in saturated KCl) at 25 mV s^{-1} in a deoxygenated solution containing $[Pt(NH_3)_4]^{2+}$ (25.6 mmol l^{-1}) at pH 10.4 and various temperatures.

Figure 3.05 (b) shows a plot of ln $\{I_D\}$ vs T^{-1} which demonstrates conclusively that at no temperature does the experimental peak current density approach the diffusion limited value. Hence, the deposition cannot be mass transport controlled.

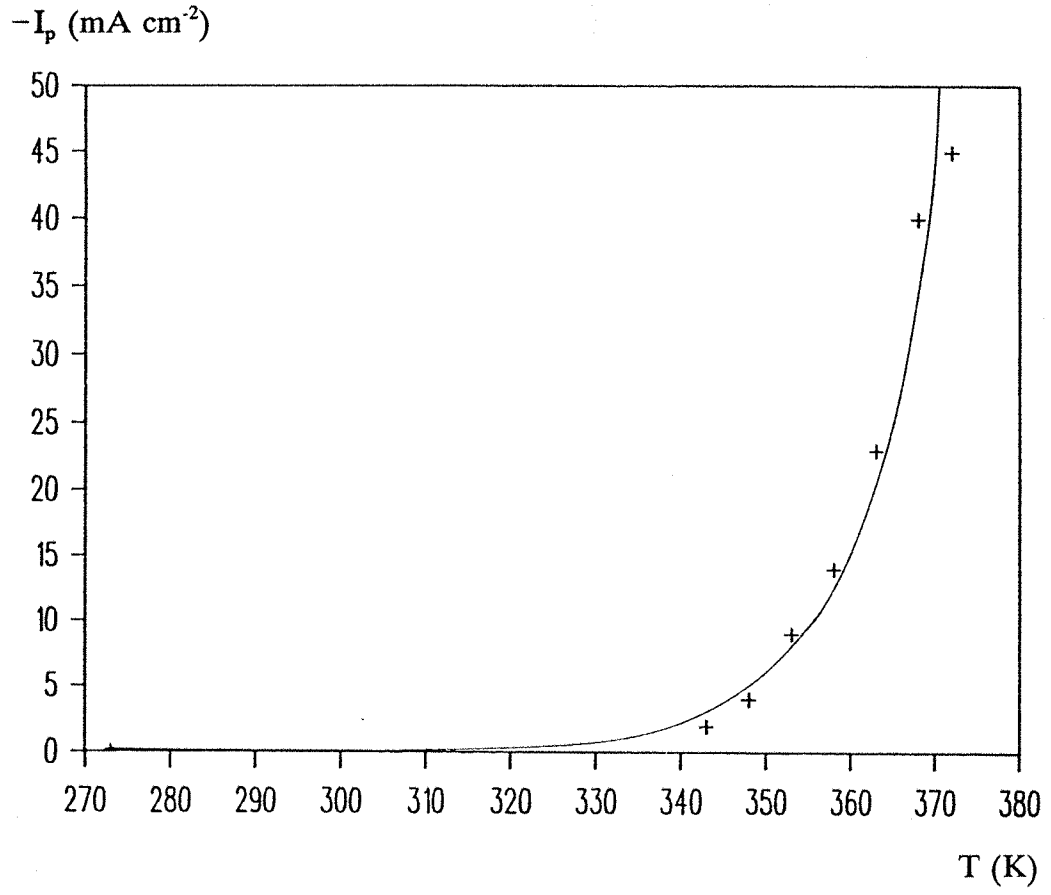

Figure 3.04:Variation of I_p(reverse mean) vs temperature using a Pt microdisc (r=12.5 μm) scanned from 0 to -1 V (vs Ag/AgCl in saturated KCl) at 25 mV s^{-1} in a deoxygenated solution containing $[Pt(NH_3)_4]^{2+}$ (25.6 mmol l^{-1}) at pH 10.4.

The pH of the Pt5Q bath, taken 60 minutes after heating commenced, became lower as the temperature increased. After adjustment to pH 10.4 all the solutions showed approximately the same drift of pH with time at all temperatures. Table 3.02 tabulates the pH readings taken during the microelectrode experiments with temperature and time.

The largest variation in pH occurred early in the experiment. This suggested that the effect was not a continuous time dependant process but rather a change in an equilibrium as a function of temperature. The magnitude of the effect was small and its origin is not yet known.

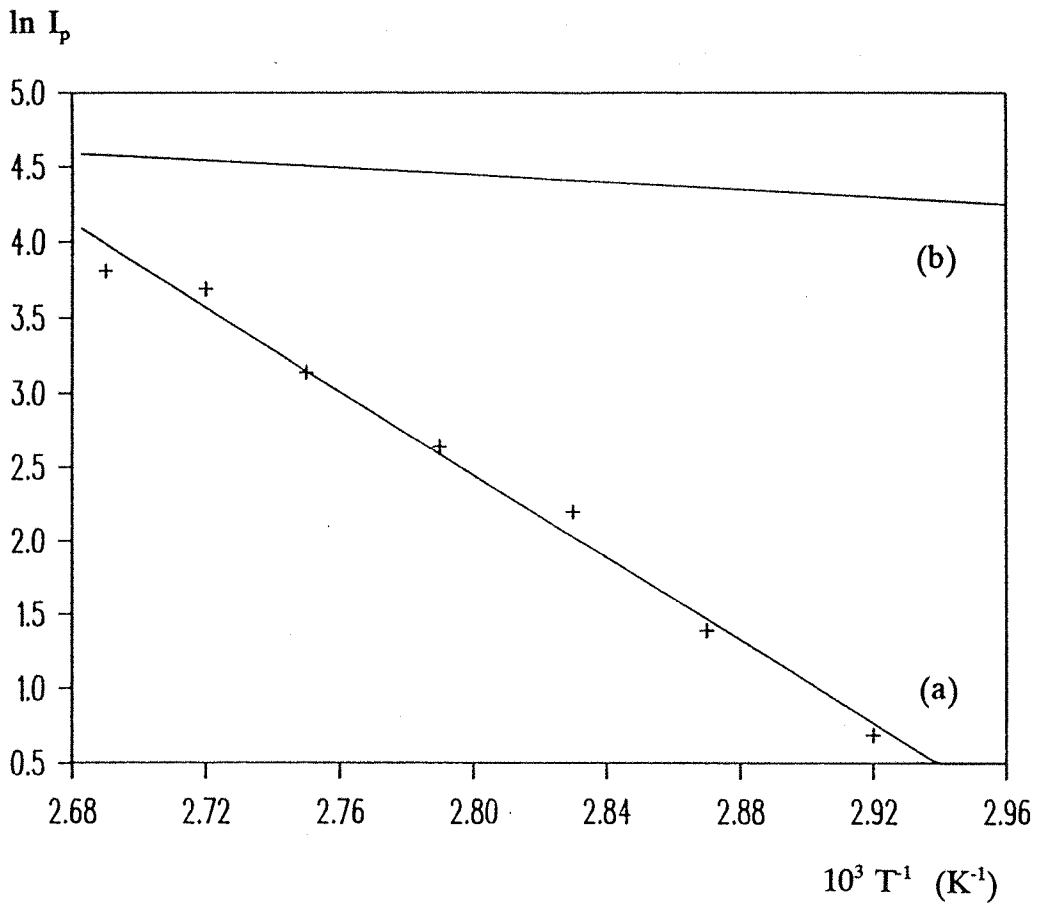

Figure 3.05 (a):Variation of ln {I_p(reverse mean)} vs T^{-1} (K^{-1}) taken from several experiments using a Pt microdisc (r=12.5 μm) scanned from 0 to -1 V (vs Ag/AgCl in saturated KCl) at 25 mV s^{-1} in a deoxygenated solution containing $[Pt(NH_3)_4]^{2+}$ (25.6 mmol l^{-1}) at pH 10.4.

(b):Variation of ln {I_D} vs T^{-1} generated by equations 3.01 and 3.02 assuming D_{293}=8.3 x 10^{-6} cm^2 s^{-1} and E_A=10 kJ mol^{-1}.

T (K)	pH before heating	pH 60 min after heating	pH after adjustment	pH 140 min after adjustment
343	10.1	10.1	10.4	10.3
348	10.1	9.9	10.5	10.3
353	10.1	9.9	10.4	10.3
358	10.1	9.8	10.5	10.4
363	10.1	9.8	10.4	10.2
368	10.1	9.6	10.5	10.1
372	10.1	9.6	10.4	10.1

Table 3.02: pH variation with time as a function of temperature for the same microelectrode experiments shown in table 3.01

3.2.3. Macro scale platinum deposition experiments from tetrakis(ammine)platinum(II) hydrogen orthophosphate

The current efficiency for platinum deposition from $[Pt(NH_3)_4]HPO_4$ (25.6 mmol l^{-1}) in aqueous Na_2HPO_4 (28.1 mmol l^{-1}) at pH=10.4 was studied as a function of temperature. The Pt5Q solution (100 cm^3, 0.49 g Pt) was deoxygenated with nitrogen whilst the temperature was increased to the selected value. Both pH and temperature readings were taken before adjusting the pH to 10.4. Platinum was deposited onto a freshly cleaned copper surface (12.5 cm^2) at 4 mA cm^{-2} for approximately 1200 s. At the end of the deposition, the exact time of deposition, the increase in mass of the cathode, pH and temperature readings were noted. At all times, the temperature before and after deposition varied ± 1 K. The percentage current efficiency from equations 3.03 and 3.04. The percentage total of platinum removed from the solution by reduction onto the cathode was calculated from equation 3.05.

$$m_t = \frac{t\ I\ A\ M}{n\ F} \qquad 3.03$$

$$CE = \frac{m_e}{m_t}\ 100 \qquad 3.04$$

$$PD = \frac{\sum_{i=1}^{n} (m_e)_i}{0.49}\ 100 \qquad 3.05$$

where:

t - time (s)

I - current density (4 mA cm^{-2})

A - cathode surface area (12.5 cm^2)

M - relative atomic mass of platinum (195.1 g mol^{-1})

n - number of electrons involved in reduction (2)

F - Faraday constant (96485 C mol^{-1})

m_t - theoretical mass increase (mg)

m_e - experimental mass increase (mg)

CE - current efficiency (%)

PD - total amount of platinum deposited to the cathode (%)

After each run the quality of the deposit was judged on three criteria; adhesion, colour and reflectivity. The last two properties were judged by eye and adhesion by bending the plated substrate twice, along the same axis, through an angle > 120°.

For each temperature 4 or 5 successive runs were carried out. Between each run the platinum concentration was not replenished but the pH was readjusted to 10.4. Table 3.03 shows the quantitative results obtained. The qualitative observations on plate quality are discussed after the table.

The main points illustrated by table 3.03 are;

1) The current efficiency jumped from 20% to 100 % between 358 and 363 K.

2) The onset of the precipitation reaction slowed with temperature and at 363 K and above no precipitate was visible even after 4 runs.

3) The current efficiency at temperatures < 358 K remained constant with decreasing platinum concentration in solution, whilst above this temperature, current efficiency decreased with decreasing platinum concentration in solution.

4) The decrease in pH in this undivided cell showed no obvious trend with temperature.

A sharp increase in current efficiency to 80% between 358 and 363 K had been seen before using a deposition current density of 6.1 mA cm^{-2} in an air saturated solution [50] but the sharp increase to 100% current efficiency over the same range shows that the limiting current density of the electroactive complex is greater than 4 mA cm^{-2}. This suggests that the rate of production of the electroactive complex is at least as fast as the rate of deposition. This does not imply an increase in concentration of the electroactive complex but rather an increase in the rate of reaction, confirming both the microelectrode and NMR studies.

In experiments at lower temperatures the solution changed from a clear colourless solution to an opaque black one and on standing a fine black precipitate fell to the base of the cell. It is not certain whether this black solid is formed at the anode, cathode, or in solution. It is insoluble in water, soluble in aqua regia and shows no IR absorbtion peaks. These properties are consistent with finely divided

T (K)	run number	change in pH	m_t (mg)	m_e (mg)	CE (%)	PD (%)	black ppt ?
343	1	-0.2	64	3	5	1	yes
	2	-0.2	80	3	4	1	yes
	3	-0.1	67	3	5	2	yes
	4	-0.1	61	3	5	2	yes
	5	-0.2	61	3	5	3	yes
348	1	-0.1	61	3	5	1	yes
	2	-0.1	66	4	6	1	yes
	3	-0.1	61	4	7	2	yes
	4	-0.1	61	4	7	3	yes
	5	-0.2	61	4	7	4	yes
353	1	-0.1	82	9	11	2	yes
	2	-0.1	61	7	11	3	yes
	3	*	61	8	13	5	yes
	4	*	63	6	10	6	yes
	5	-0.1	63	8	13	7	yes
358	1	0.0	46	9	20	2	no
	2	-0.1	61	11	19	4	yes
	3	-0.1	68	13	19	7	yes
	4	-0.1	61	12	20	9	yes
363	1	-0.2	62	62	100	14	no
	2	-0.1	61	51	84	23	no
	3	-0.1	61	42	62	32	no
	4	-0.1	63	12#	19	34	no
368	1	-0.1	68	69	101	14	no
	2	-0.3	61	63	102	26	no
	3	-0.2	62	58	92	38	no
	4	-0.1	62	52	85	48	no
372	1	-0.3	67	69	104	14	no
	2	-0.2	68	68	99	27	no
	3	-0.2	67	52	86	38	no
	4	-0.1	61	45	74	47	no

Temperature drop 2 K over this experiment.

* Readings not taken.

Table 3.03 :Current efficiency for platinum deposition from deoxygenated Pt5Q solution as a function of temperature.

platinum as the black deposit. The black solid was only observed under conditions where the cathode showed a black electroplate.

The amount of black deposit decreases as the temperature is increased and none is observed at or above 363 K where good quality deposits are observed.

At temperatures at or above 363 K a decrease in current efficiency is observed as the concentration of platinum decreases. This is to be expected as the rate of production of the electroactive complex depends on the concentration of all the platinum species previous to it. Below 363 K no decrease in current efficiency is seen since the platinum does not deposit on the cathode but falls to the bottom of the cell, however, the same trend would be expected to show itself in the decreasing mass of the black precipitate with decreasing concentration of platinum in solution.

The decrease in pH at each temperature over 20 minutes is faster than that observed in the microelectrode experiments. The only differences between the experiments are the size of the electrodes and the volume of solution involved which suggests that the decrease in pH is due to an electrode reaction. The anode reaction in the Pt5Q bath is given by equation 3.06.

$$2H_2O = O_2 + 4H^+ + 4e^- \qquad 3.06$$

Adhesion was judged to be "good" at all temperatures since no cracking of occurred with this simple bending test. Both the colour and reflectivity of the deposit from the first run improved with increasing temperature, from a dull black deposit at temperatures < 363 K to a shiny silver one at temperatures > 363 K.

At constant temperatures < 363 K there was no visible change in deposit quality as the concentration of platinum in solution decreased. At constant temperatures > 363 K the reflectivity decreased and the silver colour remained constant as platinum concentration in solution decreased.

A similar series of experiments was carried out on an oxygenated solution of

Pt5Q solution (100 cm^3). For each temperature 3 successive runs were carried out.

T (K)	run number	change in pH	m_t (mg)	m_e (mg)	CE (%)	PD (%)	grey ppt ?
343	1	0	61	3	5	1	no
	2	-0.2	71	3	4	1	no
	3	-0.1	61	3	5	2	no
348	4	-0.1	77	4	6	3	no
	5	-0.2	62	4	8	3	no
	6	-0.2	61	5	7	4	yes
353	1	-0.2	61	6	10	1	no
	2	-0.1	61	6	10	2	no
	3	-0.1	62	6	10	4	no
358	1	-0.2	61	10	16	2	no
	2	-0.2	61	10	16	4	no
	3	-0.2	61	9	15	6	no
360	1	-0.4	61	61	100	12	no
	2	-0.2	64	57	89	24	no
	3	-0.1	65	43	66	33	no
363	1	-0.2	61	60	98	12	no
	2	-0.2	61	57	93	24	no
	3	*	70	44	63	33	no
368	1	-0.2	67	67	100	14	no
	2	-0.2	61	50	82	24	no
	3	-0.2	64	30	47	30	no
372	1	-0.2	61	61	100	12	no
	2	-0.3	62	56	90	24	no
	3	-0.2	61	51	85	34	no

* Readings not taken.

Table 3.04 :Current efficiency for platinum deposition from an oxygenated Pt5Q solution as a function of temperature.

Between each run the platinum concentration was not replenished but the pH was readjusted to 10.4. Table 3.04 shows the quantitative results obtained. The qualitative observations on plate quality are discussed after the table.

The main points illustrated by Table 3.04 are;

1) The current efficiency again showed a sharp increase, from 15% to 100%, between 358 and 360 K.

2) The precipitation reaction was only observed after 6 runs on the same solution at < 348 K. At all other temperatures no precipitate was observed after 3 runs.

3) The current efficiency at temperatures < 360 K remained constant with decreasing platinum concentration in solution, whilst above this temperature, current efficiency decreased as the platinum concentration in solution decreased.

4) The decrease in pH in this undivided cell showed no trend with temperature.

The presence of oxygen in the solution had little effect on the current density measured either above or below 360 K as can be seen by comparison of tables 3.03 and 3.04. The reduction of oxygen at the cathode, equation 3.07, which occurs at more positive potentials than -0.78 V [50], was expected to decrease the current efficiency for deposition at all temperatures.

$$2H_2O + O_2 + 4e^- = 4OH^- \qquad 3.07$$

This suggests that the oxygen is reacting in some way with the deposit since it is not reduced at the cathode but this reaction neither increases nor decreases the rate of production of the electroactive complex i.e. the oxygen is acting as an additive.

The slower onset of the precipitation reaction at temperatures where the current efficiency is less than 100% must be due to oxygen blocking the precipitation reaction. The quality of the deposit is better in colour than that of the deoxygenated solution at the same low temperatures.

Despite the increase in platinum in solution at lower temperatures due to lack of precipitation the current efficiencies did not increase. At higher temperatures there was no observable difference between the oxygenated and deoxygenated solutions. This suggests that the temperature is more important than the concentration of the platinum in solution in controlling the rate of production of the electroactive complex.

The decrease in pH for the oxygenated solution was of the same order as that of the deoxygenated solution. This confirms that the oxygen did not reduce at the cathode, as in equation 3.07, since there would have been either no pH change or one to higher values.

Good adhesion was observed at all temperatures but the colour and reflectivity of each first run increased with temperature, from a dull grey at 343 K to a shiny silver at 372 K. At constant temperatures < 360 K there was no visible change in deposit quality as the concentration of platinum in solution decreased. At constant temperatures > 360 K the reflectivity decreased and the silver colour remained constant as platinum concentration in solution decreased.

Due to the absence of either a peak or wave at temperatures below 333 K it was apparent that the tetrakis(ammine)platinum(II) cation was not the reducible species, rather, a chemical step with a high activation energy forms the electroactive complex. This is consistent with one or more ligand substitution reactions producing the electroactive complex. The only potential ligands in the Pt5Q solution are the hydroxide ion or the water molecule. Since the rate is insensitive to pH [50] the ligand substitution in the rate determining step must be that of water for ammonia. The ultimate product of this is the tetrakis(aqua)platinum(II) cation which although unstable at pH 10 would only need to be present in small amounts to give the observed behaviour. For this reason the tetrakis(aqua)platinum(II) perchlorate complex was prepared and investigated.

3.3. $[Pt(H_2O)_4](ClO_4)_2$ solution

3.3.1. Characterisation and preparation of the solution

The tetrakis(aqua)platinum(II) perchlorate solution was prepared by adding stoichiometric amounts of silver perchlorate to potassium tetrachloroplatinate(II) in perchloric acid at 343 K, in the dark, under nitrogen. After seven days, the precipitated silver chloride was filtered off leaving the $[Pt(H_2O)_4](ClO_4)_2$ in solution, see equation 3.08.

$$K_2PtCl_4 + 4AgClO_4.H_2O = [Pt(H_2O)_4](ClO_4)_2 + 4AgCl\downarrow + 2KClO_4 \qquad 3.08$$

A cyclic voltammogram of the filtrate from the above reaction taken using a platinum microdisc at 293 K is shown in figure 3.06.

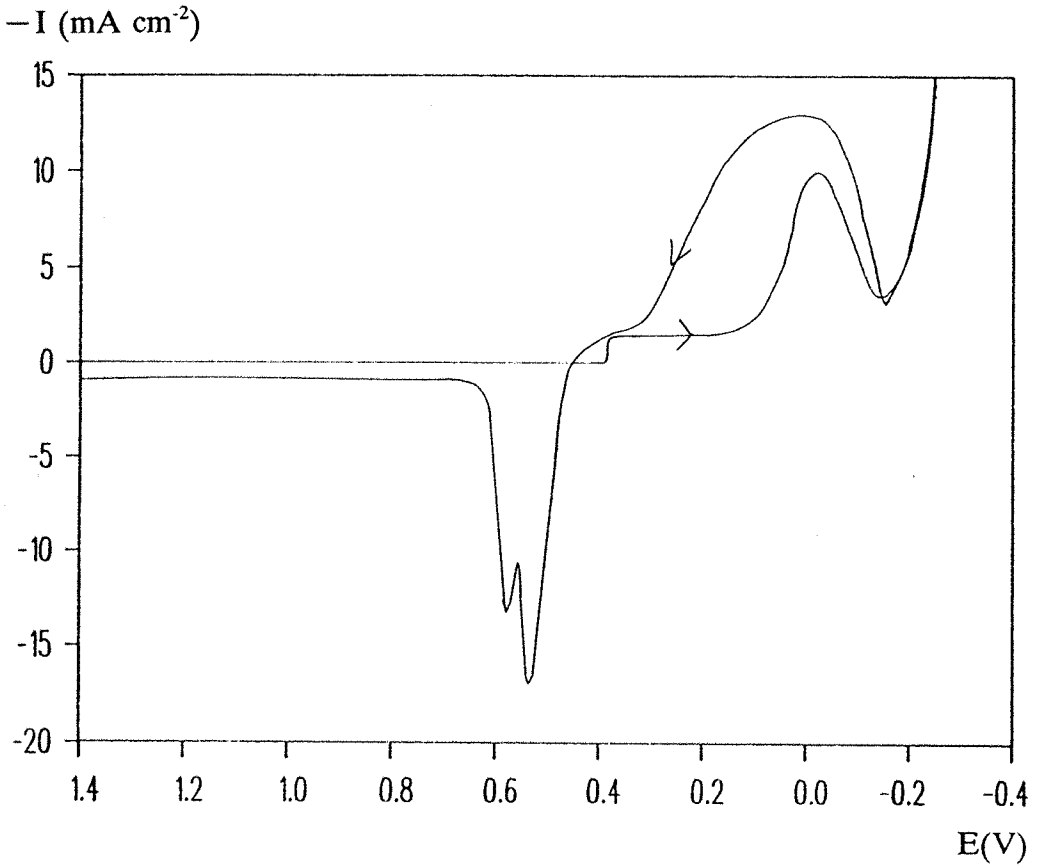

Figure 3.06:I-E curve using a Pt microdisc (r=12.5 μm) scanned from +0.7 to -0.2 V (vs Ag/AgCl in saturated KCl) at 25 mV s^{-1} in a deoxygenated solution of the filtrate from reaction 3.08

On the forward scan of this cyclic voltammogram a wave is the first feature seen, at $E_{½}$=0.39 V and I_D=-1 mA cm^{-2}, followed by a peak at E_p=-0.01 V and I_p=-10 mA cm^{-2} which is finally followed by water reduction at -0.2 V. On the reverse scan both the peak and the wave are larger due to the increased surface area of the microdisc. These features are followed by two anodic peaks at E_p=0.54 V and I_p=17 mA cm^{-2} and E_p=0.58 V and I_p=13 mA cm_{-2} and nothing further until 0.7 V where the scan stopped. Adding a few crystals of silver perchlorate monohydrate increased the height of the wave at 0.39 V showing that this was the mass transport controlled silver reduction wave. The peak at -0.01 V must therefore be the reduction of the tetrakis(aqua)platinum(II) perchlorate. At least one and possibly both of the anodic "stripping" peaks is due to silver redissolving into solution as it seems unlikely that any deposited platinum would redissolve.

The residual silver was removed by passing a current of 5 mA for t seconds through an undivided cell with a platinum foil cathode (1.5 cm × 1.5 cm) and platinum gauze anode (1.5 cm × 1.5 cm) containing the deoxygenated filtrate (100 cm^3). The time t depended on how well the solution was deoxygenated and the plating was continued until a cyclic voltammogram showed no wave at 0.39 V. Coincident with this both of the anodic peaks disappeared confirming both were silver "stripping" peaks.

The literature suggests using excess silver perchlorate in the preparation to ensure that all the $[PtCl(H_2O)_3]^+$, a thermodynamically very stable complex [71], will form $[Pt(H_2O)_4]^{2+}$. Figure 3.07 (a) shows the UV spectrum for a preparation of $[Pt(H_2O)_4](ClO_4)_2$ with a fourfold excess of Ag^+ as used by Elding and 3.07 (b) a stoichiometric amount of Ag^+ as used in this preparation. Both contain $KClO_4$ (20 mmol l^{-1}) which was not present in the reference $HClO_4$ (1000 mmol l^{-1}).

(a) There was no absorbtion in the spectrum above 600 nm. Two shoulders and a peak were clearly visible in the spectrum of the excess silver preparation solution at 382, 310 and 274 nm respectively. At wavelengths below 238 nm the solvent absorbed strongly, preventing any further comment on the spectrum. These values compare well with those in the literature 275, 312, 378 nm [65] and it was concluded that the complex was of a very high purity.

(b) This showed the same spectrum as (a) although it was not so well defined,

indicating a slightly lower purity.

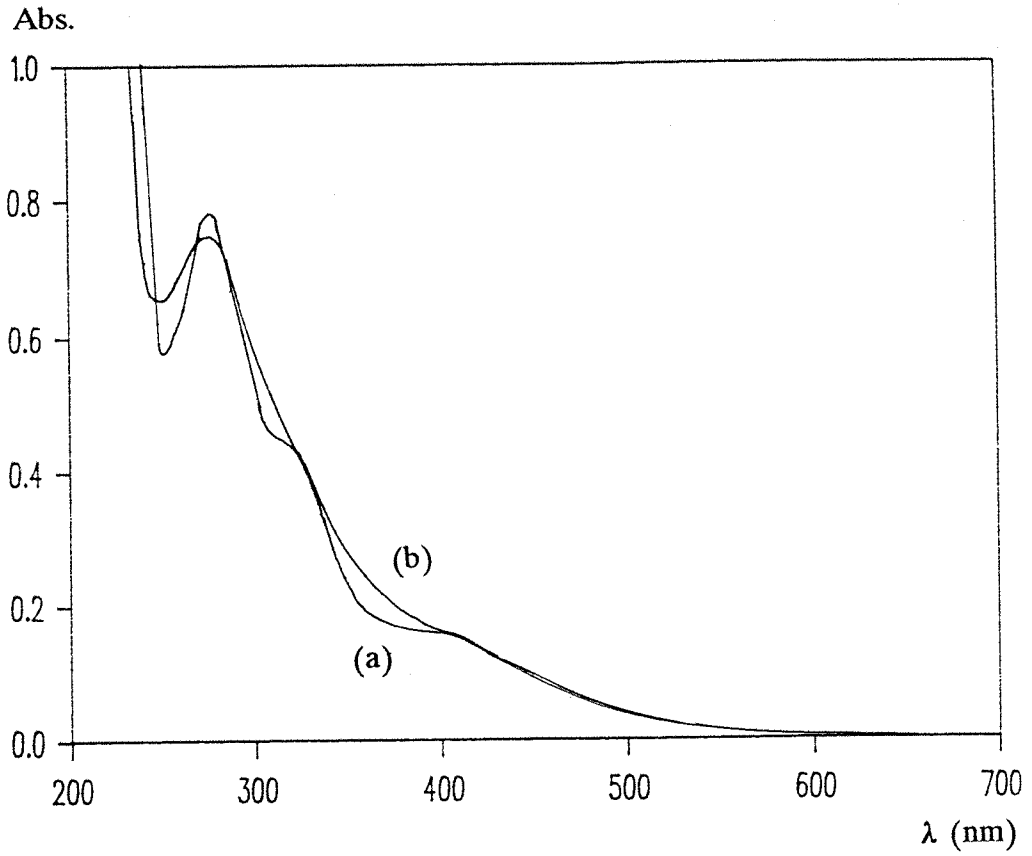

Figure 3.07:(a) UV-VIS spectrum of the filtrate from the preparation using the fourfold excess of silver perchlorate (reference $HClO_4$ (1 mol l^{-1}).
(b) UV-VIS spectrum of the filtrate from the preparation using the stoichiometric amount of silver perchlorate (reference $HClO_4$ (1 mol l^{-1})

The improvement in the spectra was not considered significant enough to spend the considerable time electroplating the silver out of solution, especially since this process often removed a large proportion of the platinum complex.

Platinum nuclear magnetic resonance spectroscopy was used to confirm the presence of $[Pt(H_2O)_4](ClO_4)_2$. Figure 3.08 shows the identical ^{195}Pt NMR spectrum obtained from both preparations.
Only one peak was observed in the range +200 to -500 ppm (reference $[PtCl_6]^{2-}$). It appeared at $\delta = 13$ ppm which agreed reasonably well with the literature [72] value

of +36 ppm.

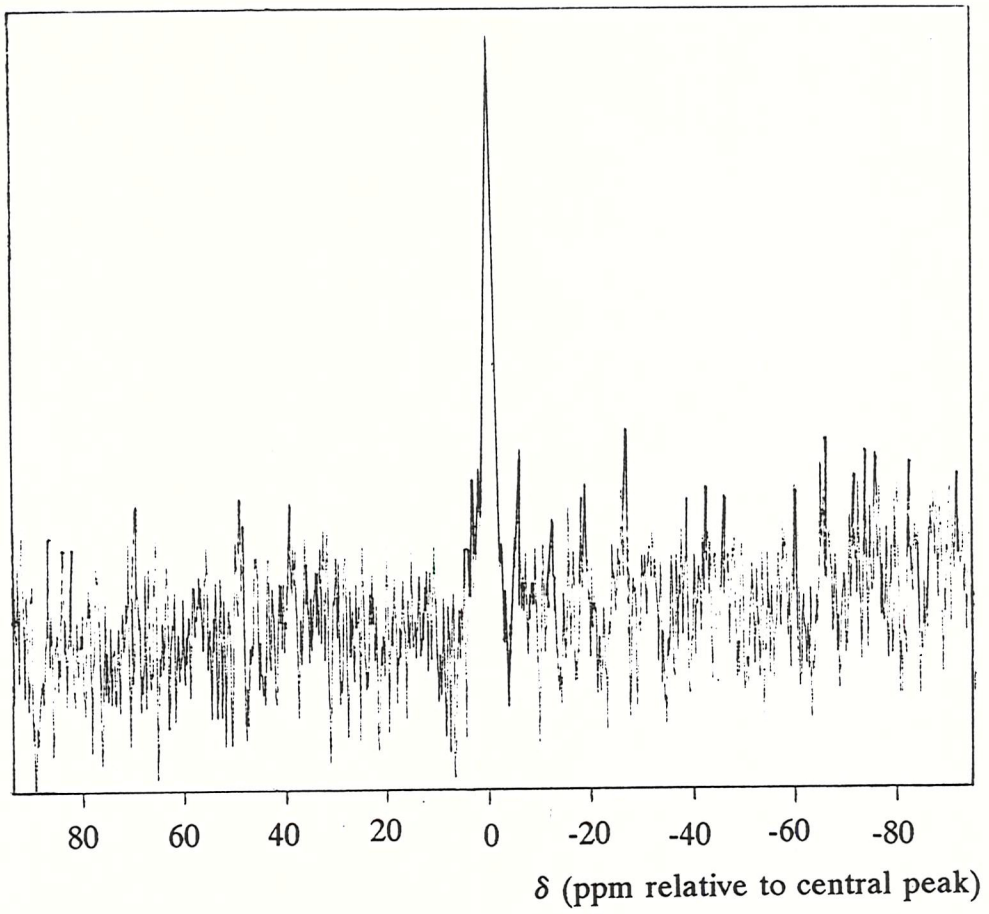

Figure 3.08: ^{195}Pt NMR spectrum of $[Pt(H_2O)_4]^{2+}$ ($\approx$50 mmol l^{-1}) in $HClO_4$ (1 mol l^{-1}) at pH 0 and 300 K after $\approx$6000 scans at 77.4 MHz δ=-13 ppm (reference $[PtCl_6]^{2-}$).

The same reference shows that both increasing the perchloric acid and sodium perchlorate concentrations affected the platinum chemical shift and so it was concluded that this peak represented tetrakis(aqua)platinum(II) perchlorate.

The exact concentration of $[Pt(H_2O)_4](ClO_4)_2$ was determined with platinum atomic absorbtion spectroscopy at 265.9 nm using an air/acetylene (fuel lean i.e. oxidising flame) with a slit of 0.7 nm. Lanthanum (III) chloride heptahydrate (AAS grade, 0.2% w/w) was added to eliminate the chemical interference effects of the high concentrations of perchlorate and chloride ions (from the sample and standard solutions respectively). The concentration of platinum in solution was obtained by

standard additions.

The platinum concentrations were always less than 10 mmol l^{-1} since both platinum and silver deposited during the electrolysis to remove silver from the filtrate. Typical values were 6.0 and 8.2 mmol l^{-1}.

A novel attempt to prepare the $[Pt(H_2O)_4]^{2+}$ by heating potassium tetrachloroplatinate(II) and trifluoromethanesulphonic acid to liberate hydrogen chloride gas, see equations 3.09 and 3.10, resulted in a mixture of products.

$$K_2[PtCl_4] + 4CF_3SO_3H = [Pt(CF_3SO_3)_4]^{2-} + 2K^+ + 4HCl\uparrow \qquad 3.09$$

$$[Pt(CF_3SO_3)_4]^{2-} + 4H_2O = [Pt(H_2O)_4]^{2+} + 4CF_3SO_3^- \qquad 3.10$$

Potassium tetrachloroplatinate(II) (2 mmol, 0.832 g) was dissolved in trifluoromethanesulphonic acid (direct from a vial 1.4 cm^3 x 1.70 g cm^{-3}=2.37 g, 17.7 mmol). The solution was continuously bubbled with nitrogen and the temperature increased to 368 K (the boiling point for this solvent is 429 K).

On heating the deep clear orange solution quickly turned grey green in colour. White fumes were seen being carried away by the nitrogen. After approx 300 s the solution turned a clear orange once more.

After 12 hours at 368 K a dark fine precipitate could be seen in the orange solution. The reaction was left to cool and the quenched with water (20 cm^3). The grey precipitate was filtered off and the filtrate examined using ^{195}Pt NMR spectroscopy. The chemical shifts of the peaks found are shown in table 3.04. The chemical shifts of the chloroaquaplatinum(II) complexes in $HClO_4$ (1 mol l^{-1}) are shown in table 3.05 [73].

chemical shift range (ppm)	number of scans	chemical shifts of any peaks seen (ppm)
+400 to -100	2000	none
-100 to -900	1645	-201, -481, -669
-900 to -1600	7500	-1187

Table 3.04 : ^{195}Pt NMR chemical shifts (relative to $[PtCl_6]^{2-}$) from the filtrate of the novel preparation at 300 K. Concentration of platinum (< 100 mmol l^{-1})

$[PtCl_4]^{2-}$	$[PtCl_3(H_2O)]^-$	$[PtCl_2(H_2O)_2]$	$[PtCl(H_2O)_3]^+$	$[Pt(H_2O)_4]^{2+}$
-1693 ppm	-1185 ppm	-810 ppm cis -636 ppm trans	-348 ppm	+31 ppm

Table 3.05 :Chemical shifts of the chloroaquaplatinum (II) complexes (40 mmol l^{-1}) (relative to $[PtCl_6]^{2-}$) in $HClO_4$ (1 mol l^{-1}).

The chemical shift of -1187 ppm is approximately that of the literature value for $[PtCl_3(H_2O)]^-$ and whilst the other three resonances maybe due to cis and trans $[PtCl_2(H_2O)_2]$ and $[PtCl(H_2O)_3]^+$ they cannot be definitely assigned. The complex $[PtCl(H_2O)_3]^+$ was assumed to be very stable with regard to further ligand substitution as no further resonances could be detected.

The grey precipitate was insoluble in water but soluble in aqua regia and was not investigated further.

3.3.2. Preliminary studies of the stability with temperature and pH of tetrakis(aqua)platinum(II) perchlorate

Sodium carbonate was added to three aliquots (10 cm^3 each) of a solution containing $HClO_4$ (1 mol l^{-1}), $[Pt(H_2O)_4](ClO_4)_2$ (8.2 mmol l^{-1}) and $KClO_4$ (20 mmol l^{-1}) until their pH was 1, 2 and 10 respectively. An additional aliquot of solution was left unadjusted at pH 0. There was no change in the colour or clarity of the solutions with increased pH compared to the original solution at pH 0.

The solutions at pH 0, 1, 2 and 10 were deoxygenated with nitrogen at 293 K and their cyclic voltammograms were recorded within 10 minutes of the pH adjustment. Figure 3.09 shows the forward scans of the cyclic voltammograms obtained at 293 K.

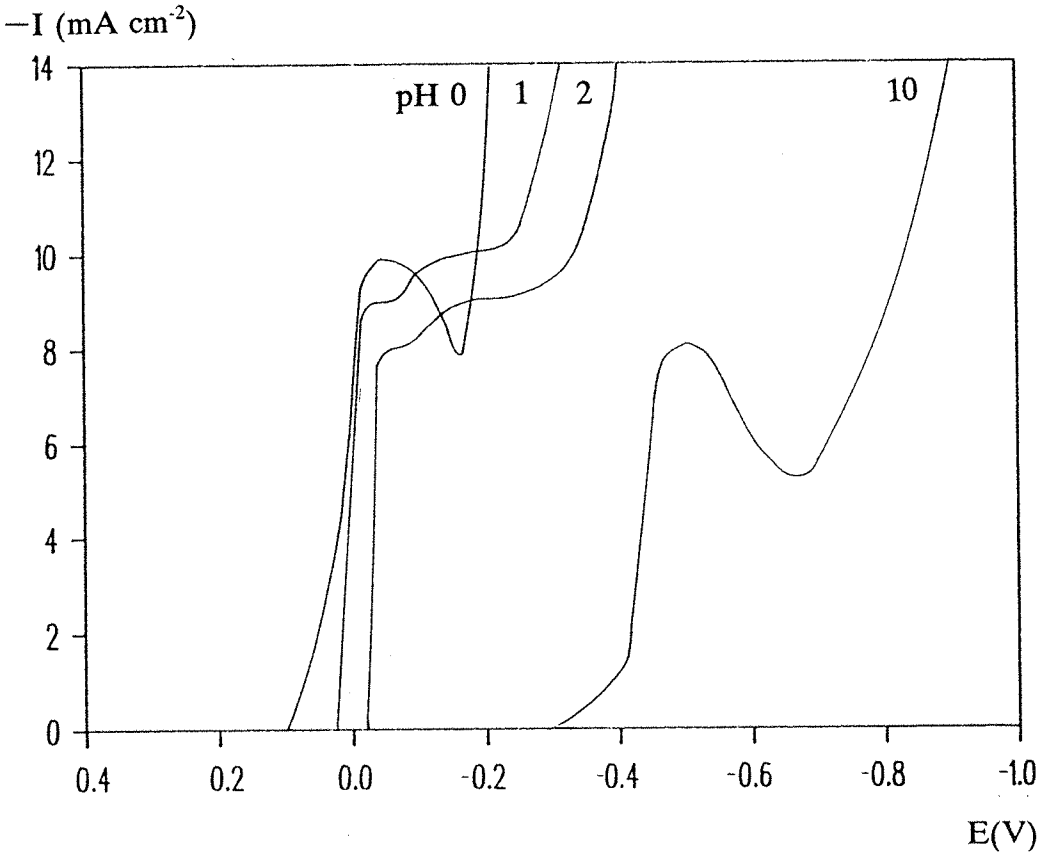

Figure 3.09:I-E curves using a platinum microdisc (r=12.5μm) from +0.38 to -0.18 V for pH 0, 1, 2 and from 0 to -1.0 V for pH 10 (vs Ag/AgCl in saturated KCl) at 25 mV s^{-1} at 293 K. The deoxygenated solution initially contained $[Pt(H_2O)_4](ClO_4)_2$ (8.2 mmol l^{-1}).

Table 3.06 tabulates the reduction potentials and the associated current densities of the waves and peaks observed.

pH	first wave		second wave		first peak	
	$E_{½}$ (V)	$-I_D$ mA cm^{-2}	$E_{½}$ (V)	$-I_D$ mA cm^{-2}	E_p (V)	$-I_p$ mA cm^{-2}
0	+0.10	10	none	none	none	none
1	+0.01	9	-0.08	1	none	none
2	-0.03	8	-0.08	1	none	none
10	none	none	none	none	-0.53	8

Table 3.06 :Data taken using a platinum microdisc (r=12.5μm) from 0.4 to -0.4 V for pH 0, 1, 2 and from 0 to -1.0 V for pH 10 (vs Ag/AgCl in saturated KCl) at 25 mV s^{-1} at 293 K. The deoxygenated solution initially contained $[Pt(H_2O)_4](ClO_4)_2$ (8.2 mmol l^{-1}).

At pH 0 there is only one wave present indicating that only one electroactive complex, $[Pt(H_2O)_4](ClO_4)_2$, is present. At both pH 1 and 2 there are two waves indicating that two electroactive complexes are present. The shift in potential of 0.09 and then 0.04 V with a 1 unit change in pH is understandable for a complex with four water ligands so the first wave was assigned to tetrakis(aqua)platinum(II) perchlorate. The second is due to another unknown complex formed by the change in pH. The fact that two waves were present implied that there is no interconversion on the timescale of the experiment which suggests that the second wave is not due to a deprotonation equilibrium. Thus, $[Pt(H_2O)_3(OH)]^+$ is unlikely to be the complex reducing at -0.08 V, however, this complex must be formed as the pH increases so it may well react to form a polynuclear complex such as $[Pt(H_2O)_3(\mu\text{-}OH)Pt(H_2O)_3]^{2+}$ which may subsequently reduce. At pH 10 only one broad peak is present implying that only one electroactive complex is present. This may be a mononuclear complex, such as $[Pt(OH)_3(H_2O)]^-$ or $[Pt(OH)_4]^{2-}$ or a polynuclear one.

These solutions were then heated to 333 K and left at this temperature for 3 days. Table 3.07 shows the qualitative data obtained during the heating of the solutions. In all the solutions with pH > 0, a fine black precipitate formed and the

colour decreased. It was observed, by eye, that as the pH increased so did the amount of precipitate and that as the amount of precipitate increased so did the extent of the decrease in the yellow colour.

The yellow colour is due to the absorption peak of $[Pt(H_2O)_4]^{2+}$ at 378 nm, a decrease in its intensity means the concentration of the complex is decreasing. This is consistent with the increasing amount of precipitate observed which is likely to be a platinum oxide, hydroxide, polynuclear hydrolysis product or platinum itself from a disproportionation reaction, already reported in alkaline (pH 14) solutions at 293 K [74].

pH	Appearance of the solution	
	after 10 minutes at 293 K	after 3 days at 333 K
0	yellow, no ppt	yellow, no ppt
1	yellow, no ppt	paler yellow than pH 0, some ppt
2	yellow, no ppt	paler yellow, more ppt than pH 1
10	yellow, no ppt	colourless, more ppt than pH 2

Table 3.07 :Qualitative observations of $[Pt(H_2O)_4](ClO_4)_2$ before and after heating to 333 K at various pHs.

The solutions were then filtered and their cyclic voltammograms recorded at 293 K. Figure 3.10 shows the forward scans obtained at 293 K.
Table 3.08 tabulates the reduction potentials and their associated current densities for the solutions after heating and cooling to room temperature.

At pH 0 there is still only one wave, $E_{½}$=0.11 V, indicating that the complex, $[Pt(H_2O)_4]^{2+}$, is unaffected by temperatures up to 333 K. At pH 1 and 2 the existence of two waves again indicates that there is no interconversion, on the timescale of the experiment, of the two platinum complexes present. At pH 1 the two waves are still observed and their combined height confirms that a small amount of a platinum species has precipitated. At pH 2, the heights of both these waves are greatly reduced whilst the amount of precipitate present increased, further confirming that the precipitate contains platinum. The first wave at pH 1 is due to

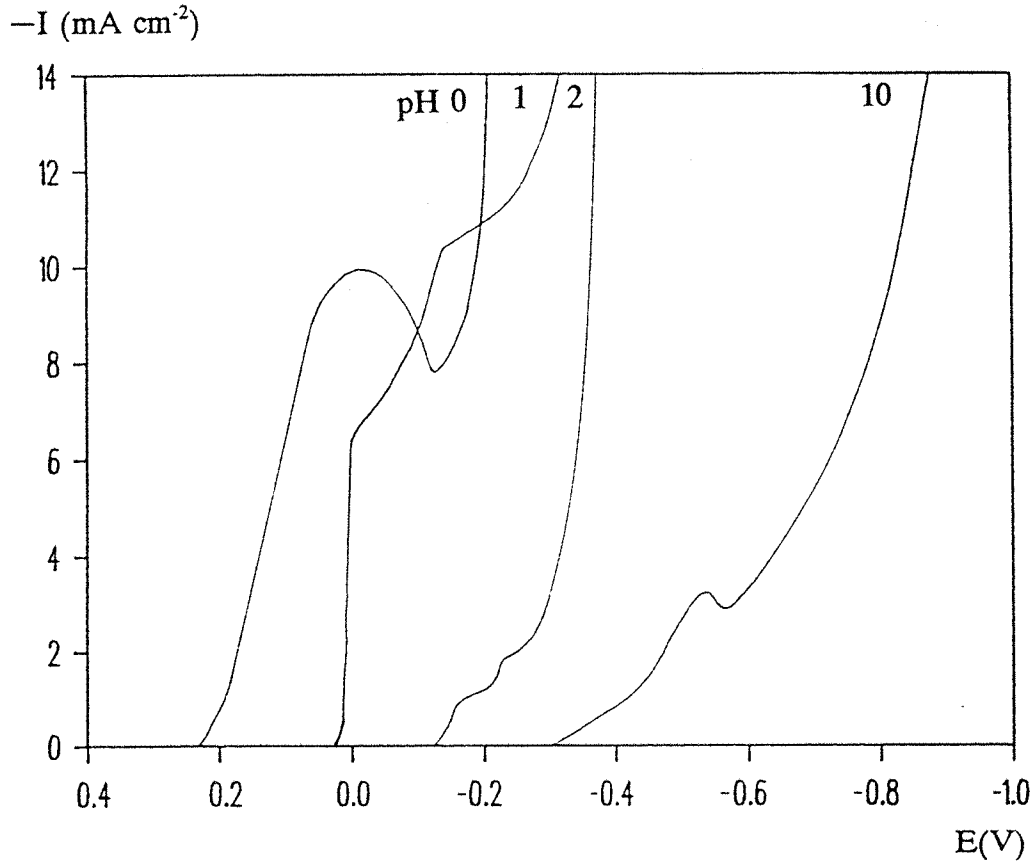

Figure 3.10:I-E curves using a platinum microdisc (r=12.5μm) from +0.38 to -0.28 V for pH 0, 1, 2 and from 0 to -1.0 V for pH 10 (vs Ag/AgCl in saturated KCl) at 25 mV s^{-1} after heating at 333 K for 3 days. The de-oxygenated solution initially contained $[Pt(H_2O)_4](ClO_4)_2$ (8.2 mmol l^{-1})

pH	first wave		second wave		first peak	
	$E_{½}$ (V)	I_D mA cm^{-2}	$E_{½}$ (V)	I_D mA cm^{-2}	E_p (V)	I_p mA cm^{-2}
0	+0.11	10	none	none	none	none
1	+0.10	6	-0.15	4	none	none
2	-0.15	1	-0.21	1	none	none
10	none	none	none	none	-0.55	1

Table 3.08 :Data taken using a platinum microdisc (r=12.5μm) from +0.38 to -0.18 V for pH 0, 1, 2 and from 0 to -1.0 V for pH 10 (vs Ag/AgCl in saturated KCl) at 25 mV s^{-1} after heating at 333 K for 3 days. The de-solution initially contained $[Pt(H_2O)_4](ClO_4)_2$ (8.2 mmol l^{-1}).

the presence of $[Pt(H_2O)_4]^{2+}$. The second wave at pH 1 and the first at pH 2 is probably due to the same polynuclear complex. The second wave at pH 2 is probably due to another polynuclear complex. At pH 10 the only peak present did not change potential implying that the complex present had not changed. Its current density, however, decreased even more than the solution at pH 2 agreeing with the observation that a larger amount of precipitate is present at pH 10 compared to pH 2.

The precipitate did not dissolve in water or hydrochloric acid (1 mol l^{-1}) but it did dissolve in warm aqua regia. This is consistent with it being finely divided platinum metal but it was not investigated further.

3.3.3. Microelectrode studies of platinum deposition from tetrakis(aqua)platinum(II) perchlorate solution

A solution containing $HClO_4$ (1 mol l^{-1}), $[Pt(H_2O)_4](ClO_4)_2$ (8.2 mmol l^{-1}) and $KClO_4$ (20 mmol l^{-1}) was deoxygenated with nitrogen at 293 K. The cyclic voltammogram for this solution was recorded using a freshly polished platinum microdisc (r=12.5 μm) from +0.6 to -0.2 V (vs Ag/AgCl in saturated KCl) at 25 mV s^{-1}. Figure 3.11 shows both the forward and reverse scans of the cyclic voltammogram at 293 K.

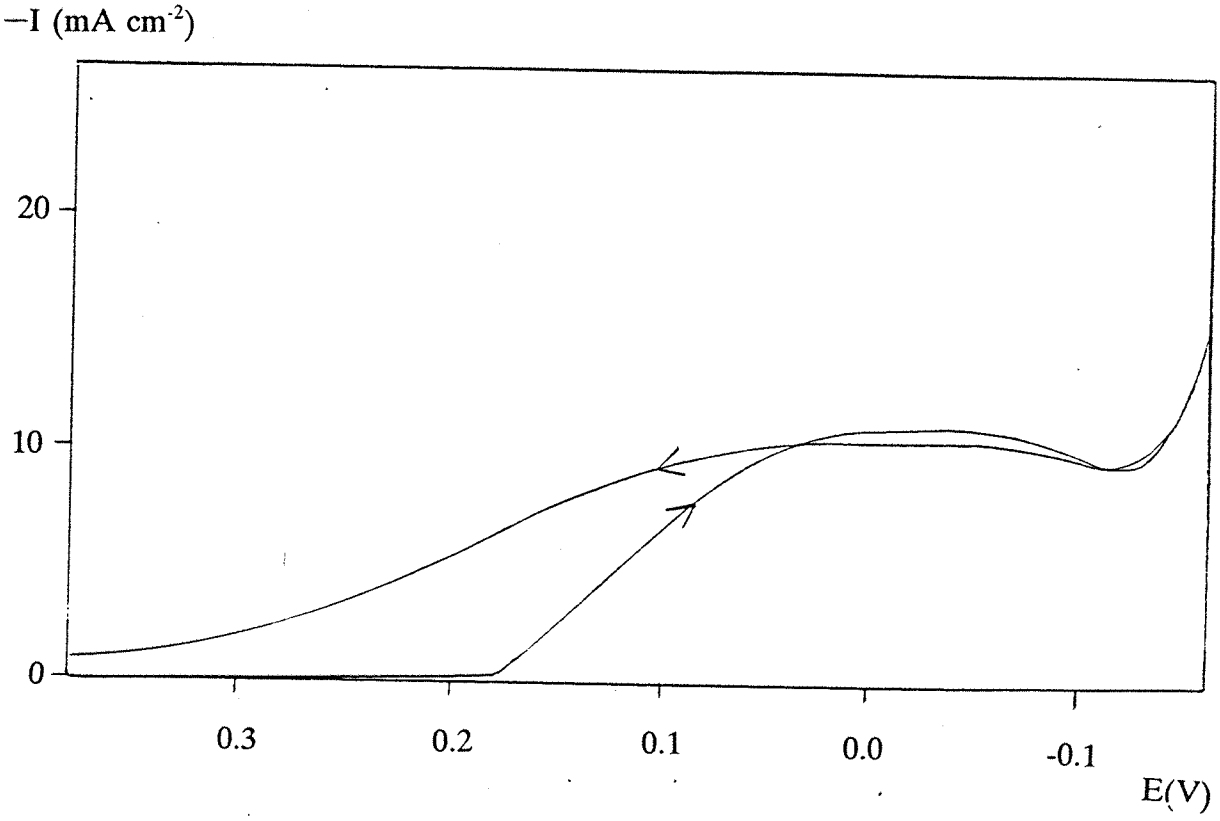

Figure 3.11:I-E curve using a Pt microdisc (r=12.5 μm) scanned from +0.6 to -0.2 V (vs Ag/AgCl in saturated KCl) at 25 mV s^{-1} in a deoxygenated solution containing $[Pt(H_2O)_4](ClO_4)_2$ (8.2 mmol l^{-1}) at pH 0 and 293 K.

The forward scan shows a wave, $E_{½}$=-0.02 V and I_D=-10 mA cm^{-2}. The diffusion limited current dipped slightly just prior to water reduction. The reverse scan showed the same behaviour but with a slightly smaller wave.

Again, the dip probably arises as platinum deposition is hindered by a blocking reaction, from -0.07 to -0.15 V. Hydrogen absorbtion has already been suggested as a possible blocking reaction for platinum deposition from the Pt5Q solution and a similar reaction may occur in acid solution.

A solution containing $HClO_4$ (1 mol l^{-1}), $[Pt(H_2O)_4](ClO_4)_2$ (8.2 mmol l^{-1}) and $KClO_4$ (20 mmol l^{-1}) was deoxygenated with nitrogen at 293 K. The cyclic voltammogram for this solution was recorded using freshly polished platinum microdisc electrodes (r=2.5, 5.0, 12.5, 25 μm) from +0.4 to -0.2 V (vs Ag/AgCl in saturated KCl) at 25 mV s^{-1}.

Figure 3.12 shows the forward scans for the i-E curves recorded for platinum microdiscs of varying radii.

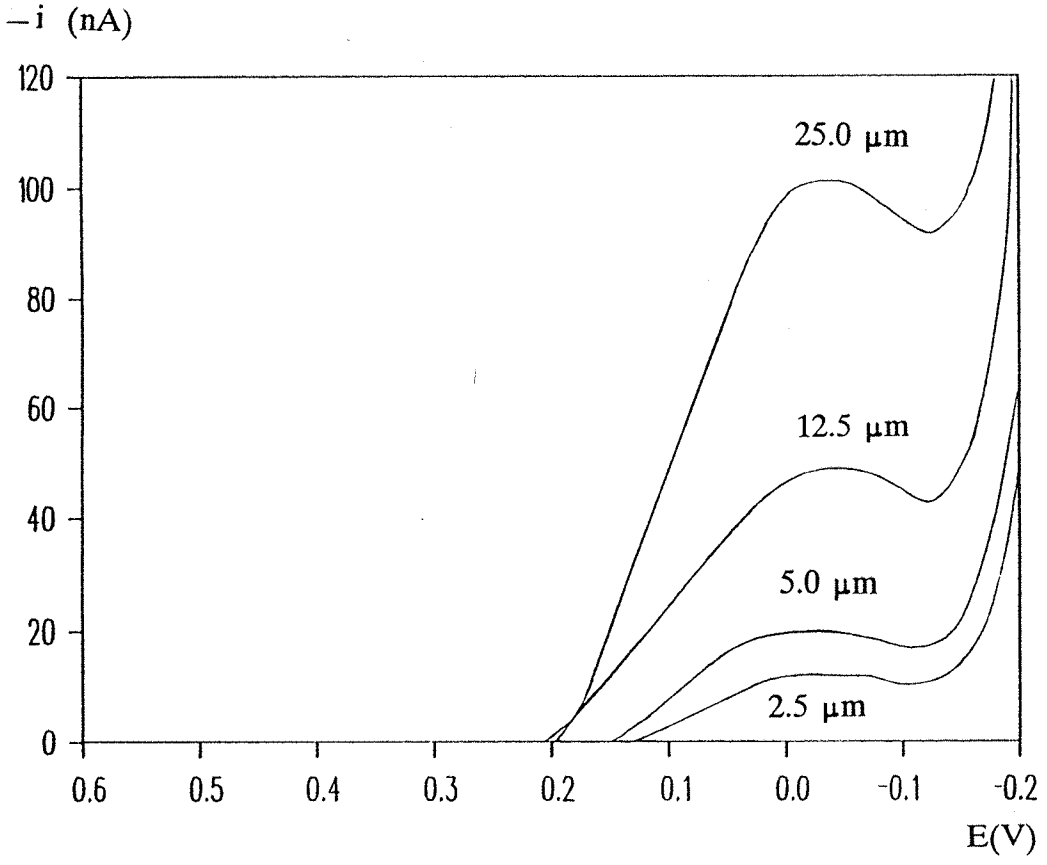

Figure 3.12:i-E curves (forward scans) of Pt microdiscs (r=2.5, 5, 12.5, 25 μm) scanned from +0.4 to -0.2 V (vs Ag/AgCl in saturated KCl) at 25 mV s^{-1} in deoxygenated $[Pt(H_2O)_4](ClO_4)_2$ (8.2 mmol l^{-1}) at pH 0 and 294 K.

Qualitatively, the i-E curves were similar in both forward and reverse scans to the curve already described in figure 3.10. From figure 3.12 it is obvious that the current increases linearly with the radius of the electrode. This is the expected behaviour for a diffusion controlled reaction at a microelectrode under steady state diffusion conditions, see equation 3.11.

$$i = 4\,n\,F\,D\,c\,r \qquad 3.11$$

where

i - current (A)

n - number of electrons involved in the deposition (2)

F - Faraday constant (96485 C mol^{-1})

D - Diffusion coefficient ($cm^2\ s^{-1}$)

c - concentration of reducible species (mol cm^{-3})

r - radius of the electrode (cm)

A plot of i vs r is shown in figure 3.13.

A linear variation of i vs r was observed, confirming that the platinum deposition reaction was mass transport controlled. The value of the diffusion coefficient calculated from the slope, 4 n F D c, was found to be 8.6×10^{-6} $cm^2\ s^{-1}$ at 294 K. This was comparable in magnitude to the diffusion coefficients of similar complexes at this temperature e.g. $D([Pd(NH_3)_2Cl_2])=8.3 \times 10^{-6}$ $cm^2\ s^{-1}$.

A solution containing $HClO_4$ (1 mol l^{-1}), $[Pt(H_2O)_4](ClO_4)_2$ (8mmol l^{-1}) and $KClO_4$ (20 mmol l^{-1}) was deoxygenated with nitrogen as it was heated to various temperatures. The cyclic voltammogram for this solution was recorded using a freshly polished platinum microdisc electrode (r=12.5 μm) from +0.6 to -0.2 V (vs Ag/AgCl in saturated KCl) at 25 mV s^{-1}. Figure 3.14 shows the cyclic voltammograms at the highest and lowest temperatures studied.

The forward scan at 293 K has already been described. The forward scan at 372 K shows a reduction wave at $E_{½}$=0.20 V and I_D=-65 mA cm^{-2} (measured at 0 V). The limiting current plateau is not as well formed as at lower temperatures.

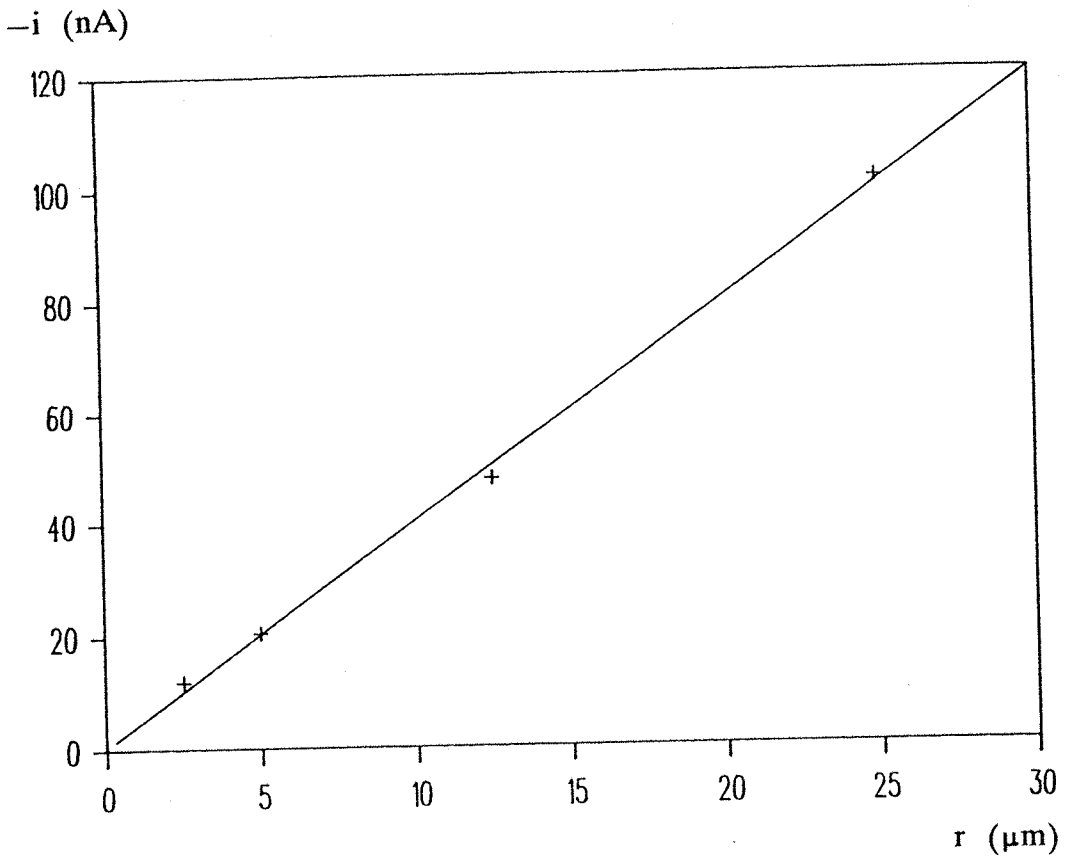

Figure 3.13:Variation of i vs r for the forward scans of platinum microdiscs (r=2.5, 5, 12.5, 25 μm) scanned from +0.4 to -0.2 V (vs Ag/AgCl in saturated KCl) at 25 mV s^{-1} in deoxygenated $[Pt(H_2O)_4](ClO_4)_2$ (8.2 mmol l^{-1}) at pH 0 and 294 K.

The following points can be made from figure 3.14.

1) The diffusion limited current, i_D, increases with temperature, see equation 3.10. Figure 3.15 shows the variation of I_D with T for all the temperatures studied.

2) The half-wave potential, $E_{½}$, steadily becomes more positive as the temperature increases, +0.12 V at 296 K compared to +0.20 V at 372 K. This is due to a quicker onset of nucleation with temperature.

3) Figure 3.16 shows an arrhenius plot of ln $\{I_D\}$ vs T^{-1} for the data shown in figure 3.15.

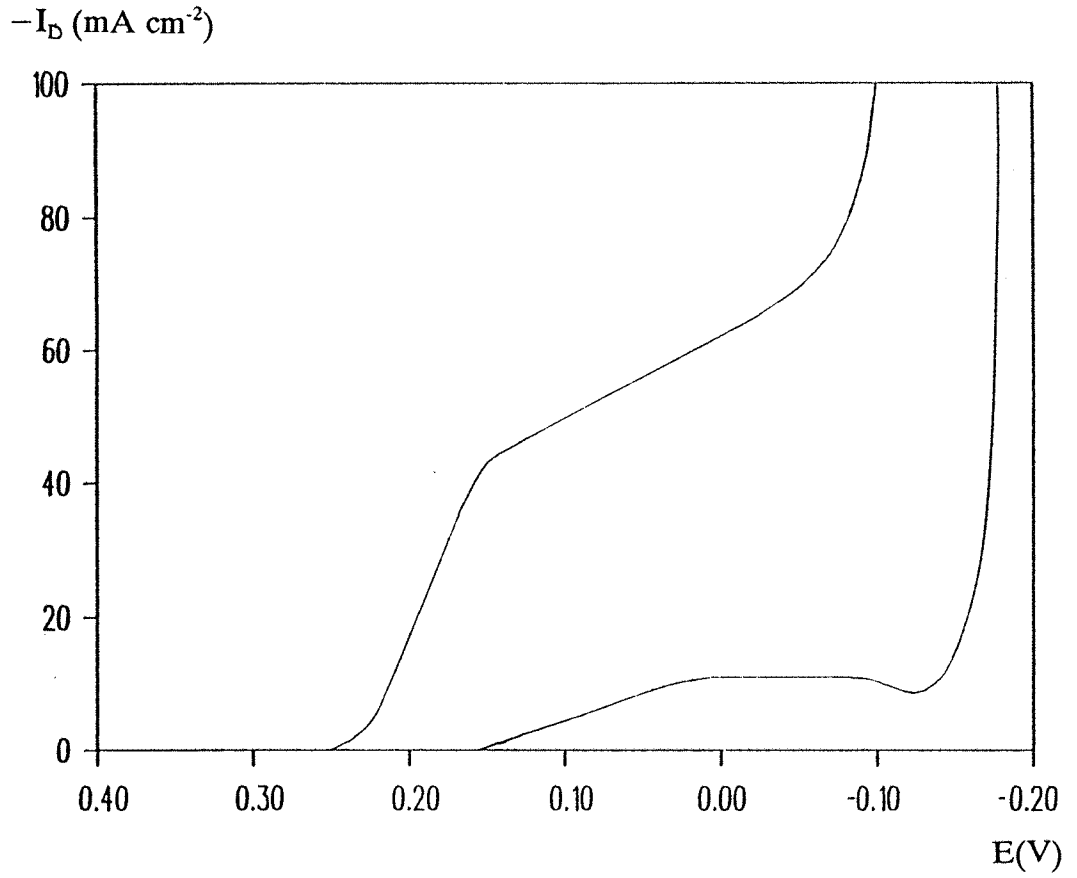

Figure 3.14:The forward scan of the I-E curve taken using a Pt microdisc (r=12.5 μm) scanned from +0.40 to -0.20 V (vs Ag/AgCl in saturated KCl) at 25 mV s^{-1} in a deoxygenated solution containing $[Pt(H_2O)_4](ClO_4)_2$ (8.2 mmol l^{-1}) at pH 0 at 2 temperatures.

The plot from figure 3.15 is a straight line, the slope of which leads to an energy of activation of 20 kJ mol^{-1}. Diffusion is known to be a process which goes through an activated state. Typically, energies of activation range from 10-20 kJ mol^{-1}.

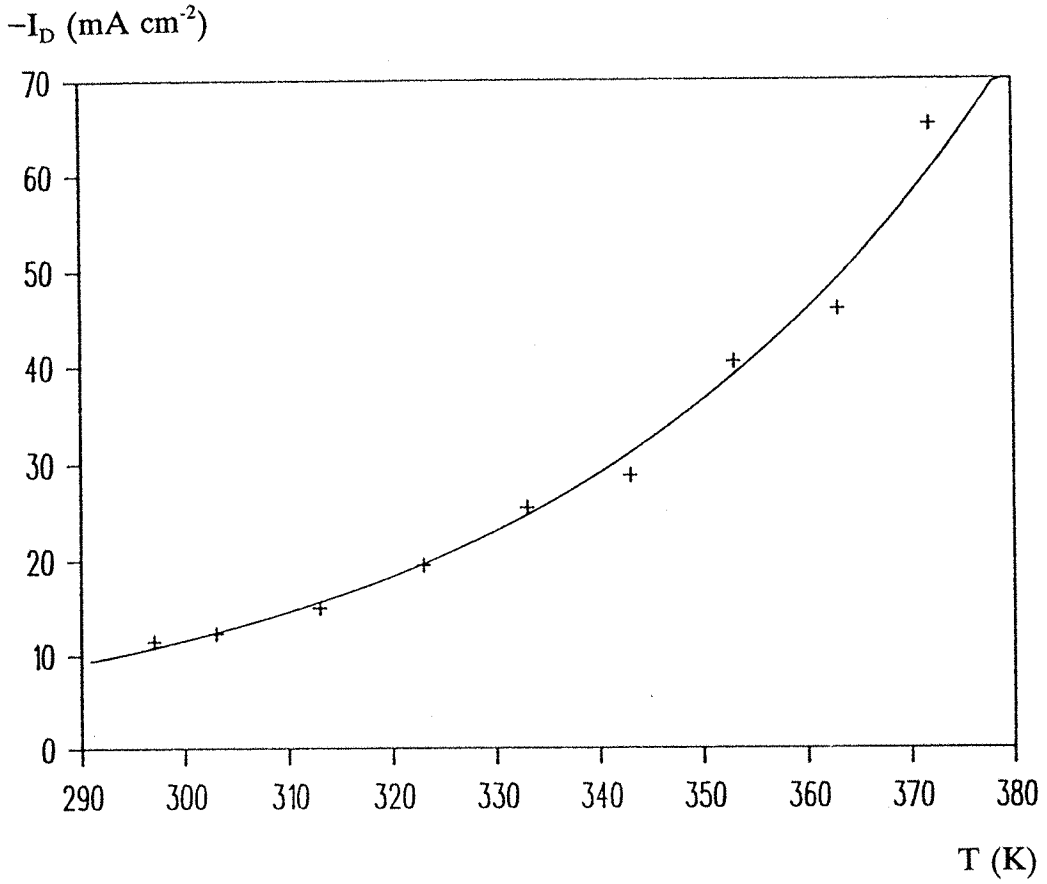

Figure 3.15:The variation of I_D vs temperature using a Pt microdisc (r=12.5 μm) scanned from +0.3 to -0.2 V (vs Ag/AgCl in saturated KCl) at 25 mV s^{-1} in a deoxygenated solution containing $[Pt(H_2O)_4](ClO_4)_2$ (8.2 mmol l^{-1}) at pH 0.

The cyclic voltammogram of a platinum microdisc (r=12.5 μm), scanned from +1.45 to -0.2 V (vs sat Ag/AgCl in saturated KCl) at 1 V s^{-1} in a solution of $HClO_4$ (1 mol l^{-1}) deoxygenated with nitrogen at 293 K, showed the characteristic and well known two adsorption and desorption peaks for hydrogen. The two adsorption peaks occur at E_p=0.02 and -0.08 V and it should be noted that the peak for weakly adsorbed hydrogen coincides with the dip in the limiting current plateau for platinum deposition.

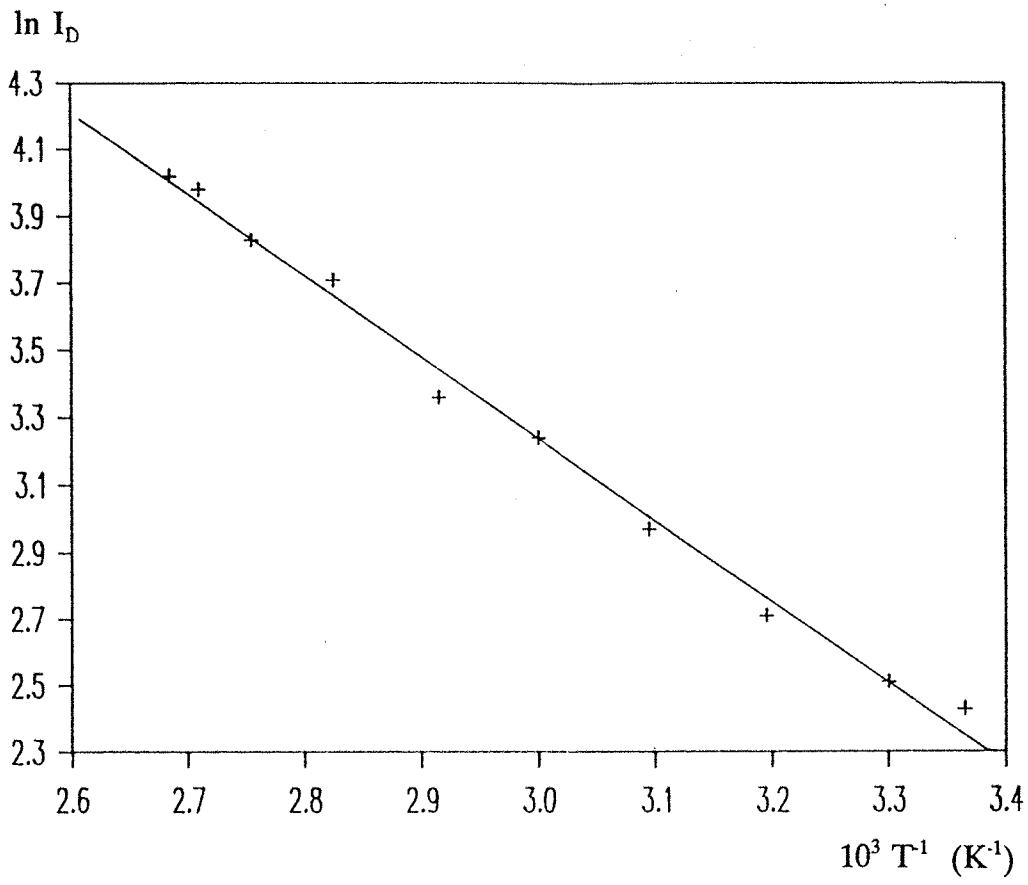

Figure 3.16:Variation of ln $\{I_D\}$ vs T^{-1} (K^{-1}) data taken from figure 3.15 which used a Pt microdisc (r=12.5 μm) scanned from +0.3 to -0.2 V (vs Ag/AgCl in saturated KCl) at 25 mV s^{-1} in a deoxygenated solution containing $[Pt(H_2O)_4](ClO_4)_2$ (8.2 mmol l^{-1}) at pH 0.

3.3.4. Macro scale platinum deposition experiments from tetrakis(aqua)platinum(II) perchlorate

The current efficiency of tetrakis(aqua)platinum(II) perchlorate was studied as a function of deposition current density.

A solution (100 cm^3) containing $HClO_4$ (1 mol l^{-1}), $[Pt(H_2O)_4](ClO_4)_2$ (8.2 mmol l^{-1}, 0.16 g) and $KClO_4$ (20 mmol l^{-1}) was deoxygenated with nitrogen at 293 K. Platinum was deposited to freshly cleaned copper surface (12.5 cm^2) at various deposition current densities, I, for various times. The copper plate was "live dipped" i.e. the plate was already charged on immersion into the solution. At the end of the deposition the exact time of deposition, t, and the increase in mass of the cathode, m_e, were noted. Both m_e and t were used to calculate the percentage current efficiency from equation 3.12 and 3.13.

$$m_t = \frac{t\ I\ A\ M}{n\ F} \qquad 3.12$$

$$CE = \frac{m_e}{m_t}\ 100 \qquad 3.13$$

where :

t - time (s)

I - current density (mA cm^{-2})

n - number of electrons involved in reduction (2)

F - Faraday constant (96485 C mol^{-1})

m_t - theoretical mass increase (mg)

m_e - experimental mass increase (mg)

CE - current efficiency (%)

For each deposition current density one run was carried out. Between each run the platinum concentration was replenished by adding a solution containing $HClO_4$ (1 mol l^{-1}), $[Pt(H_2O)_4](ClO_4)_2$ (16.4 mmol l^{-1}) and $KClO_4$ (less than 40 mmol l^{-1}). After each run the quality of the deposit was judged on the same three criteria as before, see 3.2.3. Table 3.09 shows the quantitative results obtained, the qualitative observations on plate quality are discussed after the table.

-I (mA cm^{-2})	m_t (mg)	m_e (mg)	CE (%)
0.5	21	17	81
1.0	15	8	53
4.8	36	8	22
5.4	41	8	20

Table 3.09 :Variation of current efficiency with deposition current density for a deoxygenated solution containing $[Pt(H_2O)_4](ClO_4)_2$ (8.2 mmol l^{-1}) at 293 K and pH 0.

Table 3.09 shows that as the deposition current density increases, the current efficiency decreases. At higher current densities hydrogen bubbles, from water reduction, could be seen on the workpiece, thus reducing the current efficiency for platinum deposition. This was due to the combination of a low concentration of tetrakis(aqua)platinum(II) perchlorate and a low temperature which resulted in a low mass transport controlled limiting current density. Increasing the temperature and/or the concentration of the electroactive complex would increase the current efficiency for a given deposition current density.

At all current densities, during the deposition, a flocculent pale yellow precipitate appeared in the undivided cell. This precipitate did not darken on standing in solution as does the white precipitate of $[Pt(H_2O)_2(OH)_2]$ which might be produced by a local pH change close to the cathode, see equations 3.14 and 3.15.

$$2H_3O^+ = H_2 + 2H_2O \qquad 3.14$$

$$2H_2O + [Pt(H_2O)_4]^{2+} = [Pt(H_2O)_2(OH)_2] + 2H_3O^+ \qquad 3.15$$

In the Pt5Q solution, a dull yellow solid accumulated on the anode surface during platinum deposition, although it could be removed by ultrasound or by dipping in acid. In the tetrakis(aqua)platinum(II) perchlorate solution it fell to the base of the cell. It seems certain that, in both cases, this dull yellow solid is a platinum oxide generated by the counter electrodes, see equation 3.16.

$$Pt + xH_2O = PtO_x + 2xH^+ + 2xe^- \qquad 3.16$$

The adhesion of the deposit, according to the test described in 3.2.3, was good at all current densities. As the deposition current density increased the colour of the deposit remained silver even at current efficiencies of 20%, unlike that from the Pt5Q solution. At high current efficiencies, however, several circular holes could be seen in the deposit. This was because the hydrogen evolved on the panel was not readily displaced due to the absence of any strong convection in solution at these ambient temperatures. The reflectivity decreased with increasing current density as the rate determining step for reduction became more mass transport controlled.

Hence it is the conclusion of this work that $[Pt(H_2O)_4](ClO_4)_2$ undergoes reduction to platinum in a simple electrode reaction. It is therefore possible that it is the electroactive complex in the Pt5Q bath although, because of its instability, it can only be a transient species. The $[Pt(H_2O)_4]^{2+}$ cation is stable in acid solutions and may itself be the basis for a potential electroplating bath, although corrosion of the workpiece before coating would be a problem.

Earlier work [50] reported that both $[Pt(NH_3)_3(H_2O)]^{2+}$ and cis-$[Pt(NH_3)_2(H_2O)_2]^{2+}$ at pH 10 do not reduce unless heated but no work on acid solutions was carried out. It was decided to investigate the reduction of cis-$[Pt(NH_3)_2(H_2O)_2]^{2+}$ in acid solutions.

3.4. cis-$[Pt(NH_3)_2(H_2O)_2](ClO_4)_2$ solutions

3.4.1. Preparation and characterisation

The bis(ammine)diaquaplatinum(II) perchlorate solution was prepared by reacting potassium tetrachloroplatinate(II) with ten equivalents of potassium iodide to form tetraiodoplatinate(II) in solution. This reacted with two equivalents of ammonia to precipitate bis(ammine)diiodoplatinate(II) which was filtered off and then reacted with two equivalents of silver perchlorate in perchloric acid to form bis(ammine)diaquaplatinum(II) perchlorate in solution. The reaction scheme for this preparation is given by equations 3.17, 3.18, 3.19.

$$[PtCl_4]^{2-} + 4I^- = [PtI_4]^{2-} + 4Cl^- \qquad 3.17$$

$$[PtI_4]^{2-} + 2NH_3(aq) = [PtI_2(NH_3)_2]\downarrow + 2I^- \qquad 3.18$$

$$[PtI_2(NH_3)_2] + 2AgClO_4.H_2O = [Pt(NH_3)_2(H_2O)_2](ClO_4)_2 + 2AgI\downarrow \qquad 3.19$$

A cyclic voltammogram of the filtrate from equation 3.19 taken using a platinum microdisc at 294 K is shown in figure 3.17.

No current, other than that due to the solvent, is observed at any of the potentials scanned. Hence, two conclusions can be drawn from figure 3.17;

1) The platinum complex present, $[Pt(NH_3)_2(H_2O)_2](ClO_4)_2$, is not electroactive under these conditions.

2) The solution is free of silver ion, confirming the $\approx$100% yield for reaction 3.19.

The UV-VIS spectrum of the filtrate from reaction 3.19 vs a reference of $HClO_4$ (1 mol l^{-1}) is shown in figure 3.18.

There is no absorbtion in the spectrum above 450 nm. One shoulder 318 nm and one peak 252 nm were visible before the solvent interfered at 230 nm. No literature references could be found.

Platinum nuclear magnetic resonance spectroscopy was used to confirm the presence of $[Pt(NH_3)_2(H_2O)_2](ClO_4)_2$. Figure 3.19 shows the ^{195}Pt NMR spectrum (not ^1H decoupled) obtained for a concentrated solution.

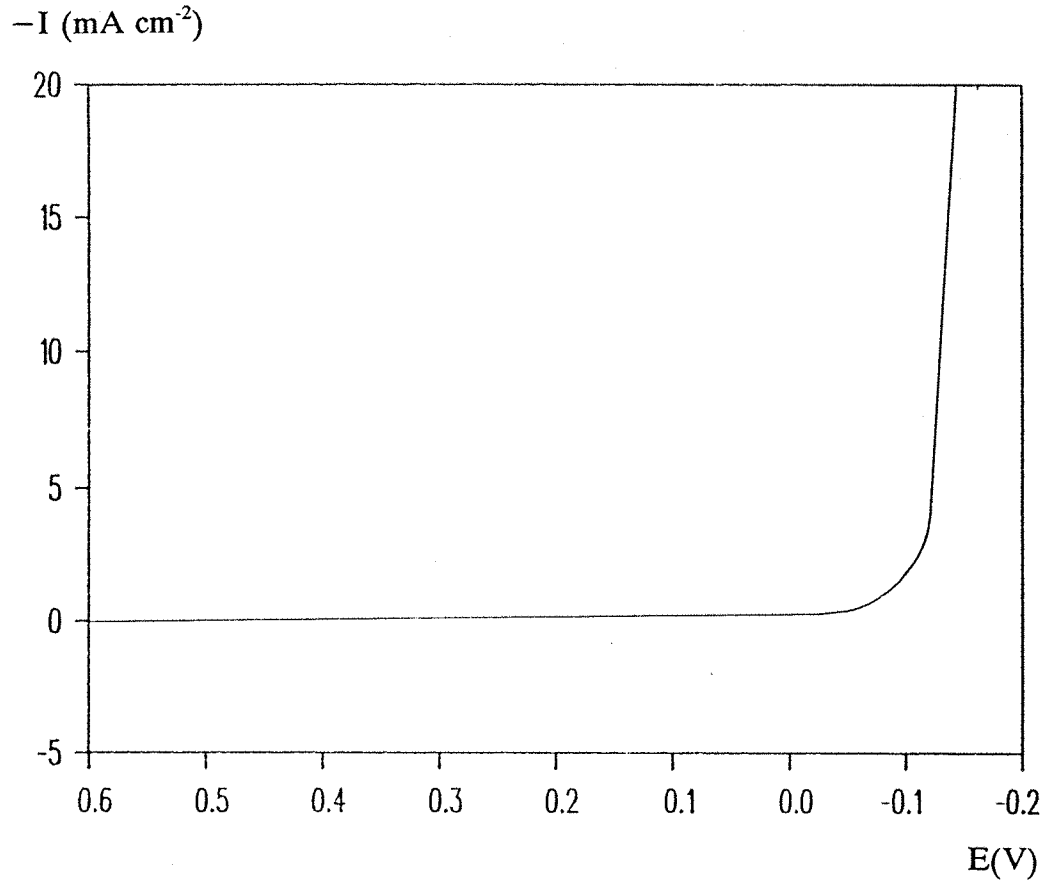

Figure 3.17:I-E curve using a Pt microdisc (r=12.5 μm) scanned from 0.6 to -0.2 V (vs Ag/AgCl in saturated KCl) at 25 mV s^{-1} in a deoxygenated solution of the filtrate from reaction 3.19 at pH 0 and 293 K.

It can be seen that this high resolution spectrum, obtained by using a high concentration and a large number of scans, shows five lines. These are the quintet of lines expected from a first order spectrum of 2 nuclei, spin 1, coupling to another nucleus, spin ½. The relative intensities should be 1:2:3:2:1 and this is observed qualitatively in figure 3.19. The chemical shift of the central line was -1555 ppm whilst the one bond coupling constant, $^{1}J(^{195}Pt\text{-}^{14}N)$, was 244 ± 5 Hz. The literature for the chemical shift is -1588 ppm for $[Pt(^{14}NH_3)_2(H_2O)_2]$ [69] and -1593 ppm for $[Pt(^{15}NH_3)_2(H_2O)_2]$ [69]. Literature values for the coupling constant are 273 Hz for $[Pt(^{14}NH_3)_2(H_2O)_2]$ [69] and 390 Hz for $[Pt(^{15}NH_3)_2(H_2O)_2]$ [69] which reduces to 280 Hz when multiplied by the ratio of the magnetogyric ratios of ^{14}N:^{15}N, 0.714.

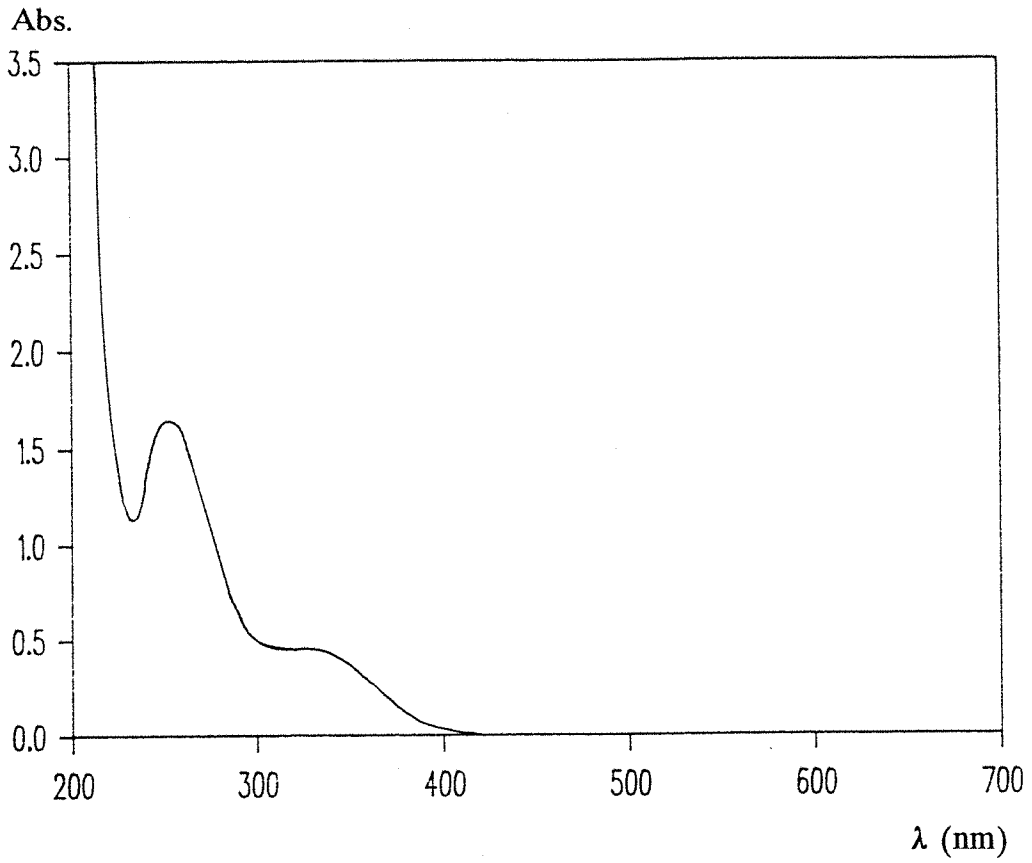

Figure 3.18:UV-VIS spectrum of the filtrate from equation 3.18 vs a reference of $HClO_4$ (1 mol l^{-1}).

The experimentally determined values do not agree as closely with the literature as those for the tetrakis(ammine)platinum(II) or the tetrakis(aqua)platinum(II) cations. This is due to the pH difference between the literature and experimental solutions affecting both the water and ammine ligands which in turn affect the chemical shift and the coupling constant. A proton decoupled spectrum would give closer agreement with the literature but these values are sufficiently close to confirm the presence of $[Pt(NH_3)_2(H_2O)_2]^{2+}$.

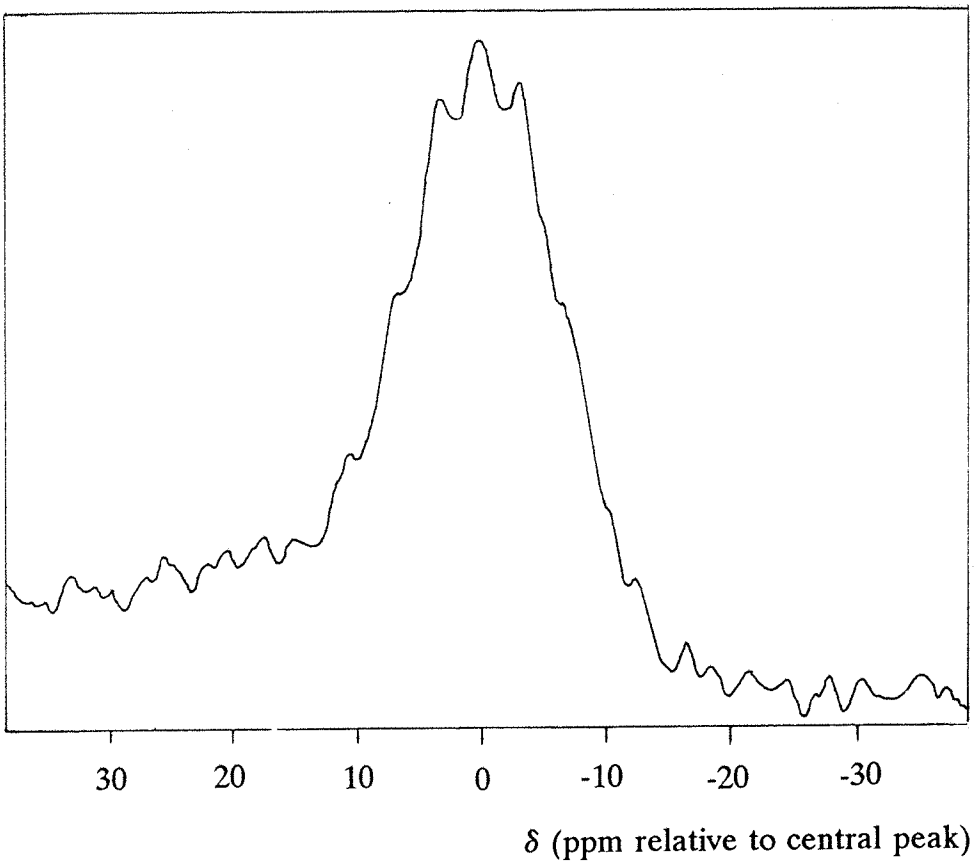

Figure 3.19: ^{195}Pt NMR spectrum of $[Pt(NH_3)_2(H_2O)_2]^{2+}$ (50 mmol l^{-1}) in $HClO_4$ (1 mol l^{-1}) at 300 K and pH 0 after ≈80000 scans at 77.3 MHz δ=-1555 ppm (reference $[PtCl_6]^{2-}$).

3.4.2. Preliminary studies of stability with temperature and pH of bis(aqua)diammineplatinum(II) perchlorate

Sodium carbonate was added to one aliquot (10 cm^3) of a solution containing $HClO_4$ (1 mol l^{-1}), $[Pt(NH_3)_2(H_2O)_2](ClO_4)_2$ (8.2 mmol l^{-1}) and $KClO_4$ (20 mmol l^{-1}) until the pH was 10. An additional aliquot of solution was left unadjusted at pH 0.

The pH adjusted solution turned brown in colour at approximately pH 2 but did not change further up to pH 10.

These two solutions were then heated to 333 K for 3 days. They were then examined by eye at 333 K and 293 K. No difference was observed in the appearance of solutions at these two temperatures. The qualitative results are shown in table 3.10.

pH	Appearance of the solution	
	after 10 minutes at 293 K	after 3 days at 333 K
0	colourless, no ppt	colourless, no ppt
10	brown, no ppt	colourless, flocculent brown ppt

Table 3.10 :Qualitative observations of $[Pt(NH_3)_2(H_2O)_2](ClO_4)_2$ before and after heating to 333 K at pH 0 and 10.

The solution at pH 0 appears stable with temperature whilst the solution at pH 10 precipitates a brown solid. This is probably a hydroxy bridged platinum ammine oligomer which are known to exist in neutral and alkaline solutions [69]. A study using ^{195}Pt NMR shows only $[Pt(NH_3)_2(OH)_2]$ in solution at pH > 10 and only $[Pt(NH_3)_2(H_2O)_2]^{2+}$ in solution at pH < 3 [75]. This implies that $[Pt(NH_3)_2(H_2O)_2]^{2+}$ is stable with respect to temperature at concentrations $\approx$8 mmol l^{-1} at pH 0 whereas $[Pt(NH_3)_2(OH)_2]$ at the same concentration at pH 10 is not.

3.5. Conclusion

The complex cation, $[Pt(NH_3)_4]^{2+}$, does not reduce directly in aqueous solution unlike its analogue, $[Pd(NH_3)_4]^{2+}$, which shows a simple diffusion controlled wave [50]. The four ammonia ligands stabilise the platinum to a greater extent than is desirable, taking the reduction potential negative of that for the solvent, water. Heating the solution increases the rate of substitution of ammonia ligands for water so increasing the rate of production of a species which is more readily reduced. Its steady state concentration is always very low since it cannot be detected spectroscopically. The only potential ligands in the Pt5Q bath are water and, less likely, hydrogen orthophosphate. All the possible equilibria for the production of the electroactive complex with water as the ligand, ignoring the possibility of oligomerisation, are shown in figure 3.20.

The horizontally shown protonation equilibria probably have extremely fast rates of reaction, since no bonds to the platinum centre are broken. These horizontal equilibria are totally pH dependant.

The diagonally shown equilibria are expected to have very slow rate of reaction since all the complexes are inert due to their d^8 electron configurations. These diagonal equilibria are unlikely to ever be reached due to the extremely slow kinetics but would probably have equilibrium constants < 1 as the Pt-N bond strength > Pt-O bond strength.

It seems likely that the complex is generated at the electrode surface and immediately reduced since bulk solutions of $[Pt(NH_3)_2(H_2O)_2](ClO_4)_2$ and $[Pt(H_2O)_4](ClO_4)_2$ give precipitates at the operating temperature and pH of the Pt5Q bath. The complex $[Pt(H_2O)_4]^{2+}$ is only stable in acid solutions but has a more positive reduction potential than water. Deposits from this complex are of a good quality and show high current efficiencies.

For a platinum plating solution to have any chance of success, it is essential for the platinum species in solution to be completely stable in the solution. The platinum species must also, however, be capable of rather facile reduction, since the Pt(II) or Pt(IV) reduction to Pt(0) must take place positive of the potential of the reduction of water to hydrogen which readily occurs on clean platinum surfaces.

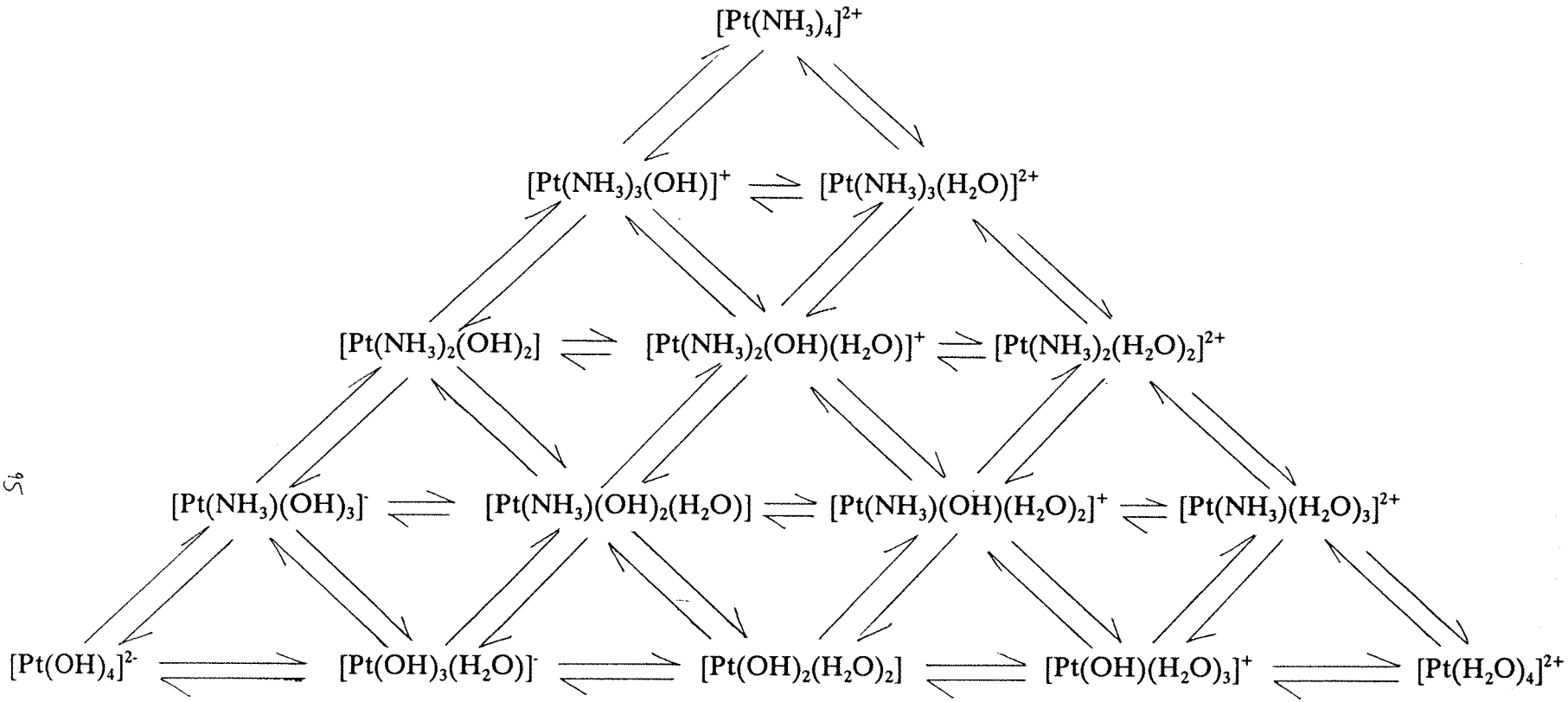

Figure 3.19:Diagrammatic scheme for the hydrolysis of $[Pt(NH_3)_4]^{2+}$ in aqueous solution, ignoring oligomerisation reactions.

To some extent these requirements are in competition; platinum ligand interactions are necessary to stabilise the platinum species but also make the reduction less favourable from a thermodynamic and, perhaps, kinetic viewpoint. The compromise of these factors determines the chemistry of the system.

Hence, the studies confirm that $[Pt(H_2O)_4]^{2+}$ is a possible transient intermediate in the reaction of $[Pt(NH_3)_4]^{2+}$ to Pt within the Pt5Q bath. The $[Pt(NH_3)_4]^{2+}$ acts as a stable source of platinum under the operating conditions of the Pt5Q bath although it is not directly electroactive itself.

The complex $[Pt(H_2O)_4]^{2+}$ in acid solution is the basis of a potential electroplating bath as it reduces in a simple, mass transport limited reduction step. Thus, its current density is a simple function of the concentration of the platinum(II) in solution and the mass transport conditions (including temperature), see equation 3.20.

$$I_L = 2\ F\ k_m\ c \qquad 3.20$$

This bath has the disadvantage that the acidic media leads to the possibility of corrosion of the substrates before they are coated with platinum. There may also be a limitation in the concentration of $[Pt(H_2O)_4]^{2+}$ which may be prepared.

Future work will therefore seek a medium with a higher pH which fulfils the requirements of a high concentration of platinum(II) which is stable in solution but also reducible. A recent paper [76] has described the preparation and spectroscopic characterisation of platinum (II) complexes with O ligands (e.g. oxalate and malonate). These seem suitable for the development of a system buffered at pH 4-6 and hence the intention is to investigate such solutions as well as polydentate inorganic oxygen anions (e.g. borate and phosphate).

4. REFERENCES

1 A. T. Kuhn, "Industrial Electrochemical Processes", (1971), Elsevier, London.

2 D. Pletcher, "Industrial Electrochemistry", 1st edition (1982), Chapman and Hall, London.

3 D. Pletcher and F.C. Walsh, "Industrial Electrochemistry", 2nd edition (1990), Chapman and Hall, London.

4 Southampton Electrochemistry Group, "Instrumental Methods in Electrochemistry", (1985), Ellis Horwood Ltd.

5 "Microelectrodes:Theory and applications", Eds. M. I. Montenegro, M. A. Queiros and J. L. Daschbach, NATO ASI series E volume 197, Kluwer Academic Publishers.

6 M. Fleischmann, L. J. Li and L. M. Peter, Electrochim. Acta., 34, (1989), 3, 459

7 L. J. Li, PhD thesis, Southampton University, (1987)

8 "Ultramicroelectrodes", Eds. M. Fleischmann, S. Pons, D. R. Rolison and P. P. Schmidt, (1987), Datatech Systems, Morganton, NC

9 J. O. Howell and R. M. Wightman, J. Phys. Chem., 88, (1984), 3915

10 E. Budevski, M. Fleischmann, C. Gabrielli and M. Labram, Electochim. Acta., 28, (1983), 925

11 M. Fleischmann, L. J. Li and L. M. Peter, Electrochim. Acta., 34, (1989), 475

12 A. M. Bond, M. Fleischmann and J. Robinson J. Electroanal. Chem., 199, (1986), 285

13 J. Ghoroghchian, F. Safarazi, T. Dibble, J. Cassidy, J.J. Smith, A. Russell, M. Fleischmann and S. Pons, Anal. Chem. 58, (1986), 2278

14 A. M. Bond, M. Fleischmann and J. Robinson, J. Electroanal. Chem., 168, (1984), 299

15 M. J. Pena, M. Fleischmann and N. Garrard, J. Electroanal. Chem., 220, (1987), 331

16 A. M. Bond and P. A. Lay, J. Electroanal. Chem., 199, (1986), 285

17 L. Cheng, A. W. Ewing, J. C. Jernigan, and R. W. Murray, Anal. Chem., 58, (1986), 852

18 L. Cheng and R. W. Murray, Inorg. Chem., 25, (1986), 3115

19 A. M. Bond and T. F. Mann, Electrochim. Acta., 32, (1987), 863

20 K. Wikiel and J. Osteryoung, J. Electrochem. Soc., 135, (1988), 1915

21 R. T. Carlin and R. A. Osteryoung, J. Electroanal. Chem., 252, (1989), 81

22 Y. Saito, Rev. Polarogr., 15, (1968), 177

23 N. N. Greeenwood and A. Earnshaw, "Chemistry of the Elements", (1984), Permagon Press, Oxford, England

24 J. de Ment and H. C. Drake, "Rarer Metals", (1949), Temple Press Ltd, London

25 S. Strelzoff and D. J. Newman, "Kirk-Othmer Encyclopedia of Chemical Technology/Nitric acid", 3rd edition, vol 15, 853-871, (1981)

26 F. A. Cotton and G. Wilkinson, "Advanced Inorganic Chemistry", 5th edition, John Wiley and Sons, New York, (1988)

27 R. G. Pearson, J. Am. Chem. Soc., 85, (1963), 3533

28 H. Irving and R. J. P. Williams, Nature, 162, (1948), 746;
J. Chem. Soc., (1953), 3192

29 J. E. Huheey, "Inorganic Chemistry", 3rd edition, (1983), Harper and Row, New York

30 G. Schwarzenbach and M. Schellenberg, Helv. Chim. Acta, 48, (1965), 28

31 C. A. Bignozzi, C. Bartocci, C. Chiorboli and V. Carrassiti, Inorganica Chim. Acta, 70, (1983), 87

32 F. Bassolo and R. G. Pearson, "Mechanism of Inorganic Reactions", 2nd edition, (1967), John Wiley and Sons, New York

33 I. I. Chenyaev, Ann. Inst. Platine, USSR, 4, (1966), 261

34 F. R. Hartley, "The Chemistry of Platinum and Palladium", (1973), Applied Science Publishers Ltd, London

35 F. Basolo, J. Chatt, H. B. Gray, R. G. Pearson and B. L. Shaw, J. Chem. Soc., (1961), 2207

36 "Science Data Book", Ed. R. M. Tennent, (1971), Oliver and Boyd, Edinburgh

37 "Multinuclear NMR", Ed. J. Mason, (1987), Plenum Press, New York

38 P. S. Pregosin, Co-ord. Chem. Rev., 44, (1982), 247

39 "NMR of newly accessible nuclei", vol 2, Ed. P. Laszlo, (1983), Academic Press, London

40 F. Basolo and R. G. Pearson, Adv. Inorg. and Radiochem., 3, (1961), 1

41 J. O. Edwards, "Inorganic Reaction Mechanisms", (1964), W. A. Benjamin, New York

42 F. Basolo, Adv. Chem. Ser., 49, (1965), 81

43 C. H. Langford and H. B. Gray, "Ligand Substitution Processes", (1965), W. A. Benjamin, New York

44 D. S. Martin, Inorg. Chim. Acta Rev., 1, (1967), 87

45 J. L. Burmeister and F. Basolo, Prep. Inorg. Reaction, 5, (1968), 1

46 "Progress in Inorganic Chemistry", vol. 13, 271, Ed. J. O. Edwards, (1971), John Wiley, New York

47 M. E. Baumgartner and Ch. J. Raub, Platinum Metals Review, 32(4), (1982), 188

48 F. Elferink, O. R. Leeuwenkamp, H. M. Pinedo and W. J. F. Van der Vijgh, J. Electroanal. Chem., 238, (1987), 297

49 T. Okubo, M. Hirota, Y. Umezawa, S. Fijiwara, J. Inorg. Nuc. Chem., 37, (1974), 573

50 R. Le Penven, PhD Thesis, University of Southampton (1991)

51 R. H. Atkinson, Trans. Inst. Met. Finish., 37, (1958/9), 7

52 F. H. Reid, Trans. Inst. Met. Finish., 48, (1970), 115; Metall. Rev., 8, (1963), 190

53 W. Keitel and H. E. Zschiegner, Trans. Electrochem. Soc., 59, (1971), 273

54 R. Lacroix and Ch. Beclier, French patent 1,356,333, (1967)

55 French patent 1,231,410, (1960); USA patent 2,984,603, (1961); USA patent 2,984,604, (1961)

56 W. Keitel and J. B. Kushner, Met. Ind. (New York), 37, (1939), 182

57 French patent 1,299,226, (1960)

58 N. Hopkin and L. F. Wilson, Platinum Metals Review, 4(2), (1960), 56

59 A. R. Powell and A. W. Scott, GB patent 363,569

60 E. C. Davies and A. R. Powell, J. Electrodepositors Tech. Soc., 13, (1937), 7

61 French patent 1,273,663, (1960)

62 W. Pfanhauser, Galvanotechnik, (1949), 870, Akademische Verlagsgesellschaft, Leipzieg

63 A. I. Vogel, "Textbook of Quantitative Chemical Analysis", 5th edition, (1989), revised by G. H. Jeffery et al, Longman Scientific and Technical, Harlow, England

64 G. Denault, PhD Thesis, University of Southampton, (1989)

65 L. I. Elding, Inorg. Chim. Acta, 20, (1976), 65

66 S. C. Dhara, Indian Journal of Chemistry, 8, (1970), 193

67 S. E. Livingstone, Synth. in Inorg. and Metal-Organic Chemistry, 1(1), (1971), 1

68 P. E. Skinner, Platinum Metals Review, 33(3), (1989), 102

69 C. J. Boreham, J. A. Broomhead and D. P. Fairlie, Aust. J. Chem., 34, (1981), 659

70 T. G. Appleton, J. R. Hall and S. F. Ralph, Inorg. Chem., 24, (1985), 4685

71 L. I. Elding, Acta Chem. Scand., 24, (1970), 1331

72 T. G. Appleton, R. D. Berry, C. A. Davis, J. R. Hall and H. A. Kimlin, Inorg. Chem., 23, (1984), 3514

73 O. Groning and L. I. Elding, Inorg. Chem., 28, (1989), 3366

74 T. G. Appleton, J. R. Hall, S. F. Ralph and C. S. M. Thompson, Inorg. Chem., 23, (1984), 3521

75 T. G. Appleton, J. R. Hall, S. F. Ralph and C. S. M. Thompson, Inorg. Chem., 28, (1989), 1989

76 S. O. Dunham, R. D. Larsen and E. H. Abbott, Inorg. Chem., 30, (1991), 4328